Lawrence Berkeley Laboratory
UNIVERSITY OF CALIFORNIA

Materials & Molecular
Research Division

Presented at the American Chemical Society Symposium, Washington, DC, September 9-14, 1979; also to be published in the Proceedings

NUCLEAR MAGNETIC RESONANCE STUDIES OF URANOCENES

Wayne D. Luke and Andrew Streitwieser, Jr.

December 1979

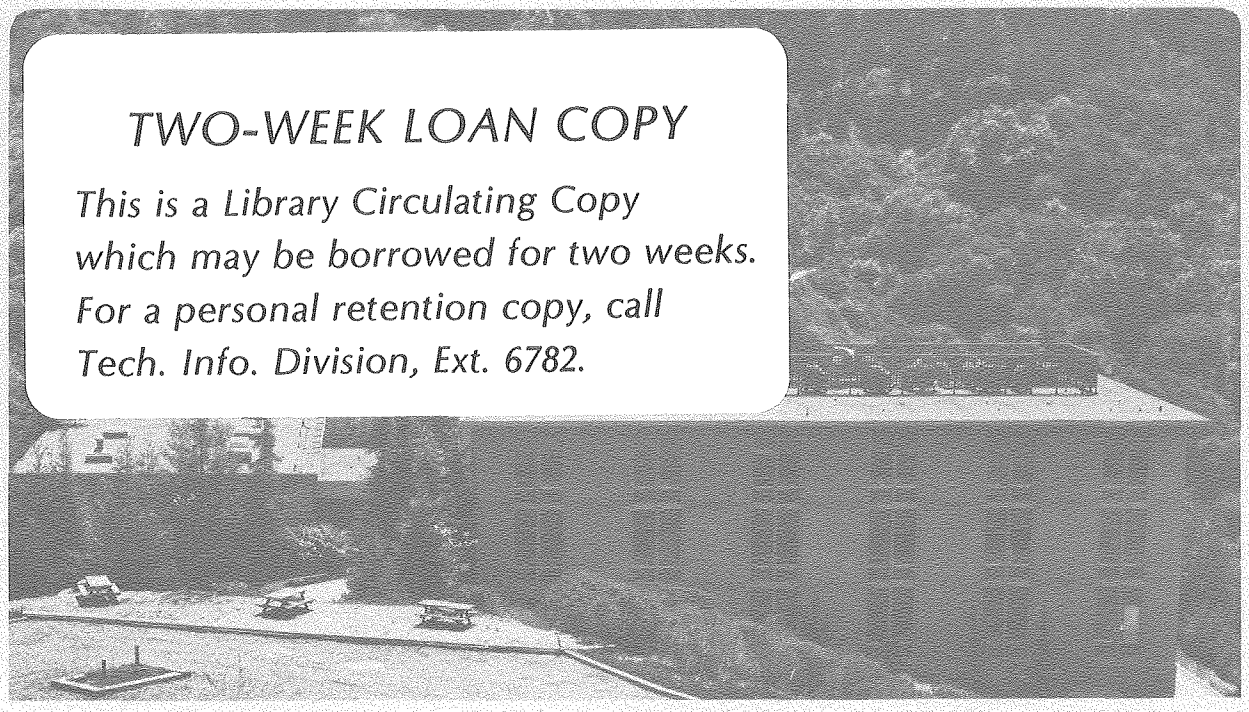

Prepared for the U.S. Department of Energy under Contract W-7405-ENG-48

DISCLAIMER

LBL-10432

NUCLEAR MAGNETIC RESONANCE STUDIES OF URANOCENES

Wayne D. Luke and Andrew Streitwieser, Jr.

Department of Chemistry and Materials & Molecular Research Division, University of California, Berkeley, California 94720

Contents

I. Introduction and Historical Background

In the past several years a substantial amount of work has been devoted toward evaluation of the contact and pseudocontact contributions to the observed isotropic shifts in the ^1H nuclear magnetic resonance (NMR) spectra of uranium(IV) organometallic compounds (1-15). One reason for interest in this area arises from using the presence of contact shifts as a probe for covalent character in the uranium carbon bonds in these compounds. Several extensive ^1H NMR studies on Cp_3U-X compounds (10-13) and less extensive studies on uranocenes have been reported (5,6,14,15). Interpretation of these results suggests that contact shifts contribute significantly to the observed isotropic shifts. Their presence has been taken as indicative of covalent character of metal carbon bonds in these systems, but agreement is not complete (2). In this paper we shall review critically the work reported on uranocenes in the light of recent results and report recent work on attempted separation of the observed isotropic shifts in alkyluranocenes into contact and pseudocontact components.

A. Theory. A detailed derivation of the theory behind paramagnetic shifts in the NMR of paramagnetic compounds, or a complete review of the literature concerning separation of observed isotropic shifts into contact and pseudocontact components is well beyond the scope of this paper. Several books and reviews of these subjects are available (16-21).

The presence of a paramagnetic metal in organometallic compounds significantly influences the NMR spectrum of ligand nuclei. Changes in nuclear relaxation times and changes in resonance frequency are the two principal effects arising from interaction between the unpaired electrons on the metal and ligand nuclei. Nuclear relaxation times are shortened due to increased spin-spin relaxation and result in increased linewidths of the resonance signals. In some compounds this broadening of the resonance signals is large enough to preclude their observation.

The coupling of the unpaired electrons with the nucleus being observed generally results in a shift in resonance frequency that is referred to as a hyperfine isotropic or simply isotropic shift. This shift is usually dissected into two principal components. One, the hyperfine contact, Fermi contact or contact shift derives from a transfer of spin density from the unpaired electrons to the nucleus being observed. The other, the dipolar or pseudocontact shift, derives from a classical dipole-dipole interaction between the electron magnetic moment and the nuclear magnetic moment and is geometry dependent.

Expressions for the contact shift vary depending on the assumptions made. One common form is (22)

$$\delta_{CONTACT} = \frac{A_i g_e^2 \beta_e^2 S(S+1)}{3 g_N \beta_N kT} \quad (1)$$

where A_i is the hyperfine coupling constant, g_e is the rotationally averaged electronic g value, β_e is the Bohr magneton, g_N and β_N are the corresponding nuclear constants and S is the spin of the unpaired electrons. For actinide organometallics in which crystal field splitting is small compared the separation between electronic states and characterized by quantum number J, but large compared to kT, the contact shift may be expressed as (12):

$$\delta_{CONTACT} = \frac{A_i (g_J - 1)\chi}{N g_J \beta_e g_N \beta_N} \quad (2)$$

in which χ is the magnetic susceptibility.

The pseudocontact shift may be expressed as (20, 23-26):

$$\delta_{PSEUDOCONTACT} = \frac{\chi_z - 1/2(\chi_x + \chi_y)}{3N} \frac{3\cos^2\theta - 1}{R^3} + \frac{(\chi_x - \chi_y)}{2N} \frac{\sin^2\theta \cos 2\psi}{R^3} \quad (3)$$

in which χ_x, χ_y and χ_z are components of the magnetic susceptibility, and the coordinate system is shown in Fig. 1.

The total isotropic shift is the sum of the two components:

$$\delta_{ISOTROPIC} = \delta_{CONTACT} + \delta_{PSEUDOCONTACT} \quad (4)$$

In this paper we define all shifts upfield from TMS as negative and all shifts downfield from TMS as positive. This is the modern accepted convention.

B. NMR of Uranium(IV) Organometallic Compounds. Current interest in the NMR of U(IV) organometallic compounds has been concerned with the relative contributions of contact and pseudocontact shifts to the observed isotropic shifts. Much of this interest arises from the possible presence, and relative role of covalency in ligand metal bonds in organoactinide compounds. Ideally, if the isotropic shifts in U(IV) compounds can be factored into contact and pseudocontact components, the contact shift can be correlated with electron delocalization and bond covalency.

From an experimental point of view, the ^1H NMR spectra of U(IV) compounds are ideally suited to such analysis. In general,

the isotropic shifts are less than ± 100 ppm, which is small compared to shifts observed in many transition metal complexes. The linewidths for protons on carbons directly bonded to uranium are less than 50 Hz and rapidly decrease for protons on carbons not directly bonded to the metal atom, so that J-J coupling is often observed. A review of early work on the ^{1}H NMR spectra of U(IV) compounds apepared in 1971 (7).

1. Triscyclopentadienyl uranium(IV) compounds. The ^{1}H NMR resonance of the cyclopentadienyl ligand in Cp_4U is shifted -19.27 ppm upfield from the corresponding resonance in diamagnetic Cp_4Th at room temperature. The interpretation of this shift involved some early controversy (1,2,4,10). Moreover, a wide variety of Cp_3U-X compounds has been prepared and extensive studies on their ^{1}H NMR spectra have been reported. Some confusion exists in comparing the isotropic shifts reported in the literature. Some shifts are reported referenced relative to various solvents while others are referenced relative to the corresponding thorium compound instead of the universal standard TMS. To facilitate comparison the reported shifts have been referenced to TMS and are recorded in Table I.

Assuming axial symmetry along the U-X bond, the isotropic shifts for compounds 3, 7-16 and 25 have been factored into contact and pseudocontact components. In the rigid cholesteroloxy ligand, 25, Fischer and co-workers (11) showed the ratio of the geometry factors $(3\cos^2\text{-}1)/R^3$ for the A-ring protons in the β and γ-positions to be equal to the ratio of the isotropic shifts, whereas gross deviations occurred when the α-positions were compared. This implies that all of the isotropic shifts except those in the α-position arise purely from pseudocontact-type interactions whereas both pseudocontact and contact interactions contribute to the α-proton isotropic shifts. The isotropic shifts were factored into contact and pseudocontact components. Taking the average geometry factor, (G_r), for the ring protons as -5.49 x 10^{-22} cm^{-3}, the calculated pseudocontact and contact shifts at room temperature are -6.4 ppm and -17.6 ppm, respectively. The approximate invariance of the ring proton isotropic shifts in all of the alkoxy substituted compounds suggests that there is no great fluctuation in the molecular anisotropy throughout this series.

Marks and co-workers (12) have studied the alkyl substituted compounds 7-16. Assuming that INDO/2 molecular orbital calculations on alkyl radicals can reasonably predict experimental electron-nuclear hyperfine coupling constants, a_i, they have calculated the a_i values for each of the alkyl substituents. Taking the ratio of the contact shifts of the ortho positions in 7 and vinylic position in 16 as equal to the ratio of calculated a_i values and the ratio of the geometry factors as equal to the ratio of pseudocontact shifts, Marks and co-workers could solve for the contact and pseudocontact shifts in 7 and 16. Factoring the

Table I

The ^1H NMR Resonances of Cp_3U-X Compounds

δ ppm from TMS

	X		Temp	Solvent	Ref.
1	Cp	-13.96	25	THF	1,7,10
2	F	-6.46	25	Benzene	7,10,27
3	Cl	-3.40	25	Benzene	7,10,13,27
4	Br	-3.65	25	Benzene	7,10,27
5	I	-4.28	25	Benzene	7,10,27
6	BH_4	-6.53	25	Benzene	3,7
7	C_6H_5	-3.26	25	Benzene	12,28
8	CH_3	-2.76 -194.76(CH_3)	25	Benzene	12
9	n-C_4H_9	-3.06	25	Benzene	12
10	i-C_3H_7	-3.66 -11.46(CH_3) -20.36(γ) -26.36(β) -192.76 (α)	25	Benzene	12
11	t-C_4H_9	-4.16 -15.96(CH_3)	25	Benzene	12
12	neopentyl	-4.36 -14.86(CH_3) -184.76(CH_2)	25	Benzene	12
13	allyl	-2.76 -30.96(CH) -118.76(CH_2)	25	Benzene	12
14	vinyl	-2.06 31.64(β-trans) -9.76(β-cis) -156.36(α)	25	Benzene	12
15	cis-2-butenyl	-3.36 -12.56(α-CH_3) -15.36(H) -35.06(β-CH_3)	25	Benzene	12
16	Trans-2-butenyl	-3.46 30.74(H) -25.76(β-CH_3) -26.36(α-CH_3)	25	Benzene	12
17	C_6F_5	-3.66	25	Benzene	12
18	OCH_3	-17.06 52.54(CH_3)	RT	Benzene	7,29
19	OC_2H_5	-18.36 59.04(OCH_2) 16.84(CH_3)	RT	Benzene	7,29

Table I (cont.)

	X		Temp	Solvent	Ref.
20	O-n-C_4H_9	-17.86 57.84(OCH_2) 17.04(ε) 8.94(γ) 4.58(CH_3)	RT	Benzene	7,29
21	O-i-C_3H_7	-18.56 121.94(OCH_2) 17.84(CH_3)	RT	Benzene	7,29
22	O-t-C_4H_9	-19.36 19.64(CH_3)	RT	Benzene	7,29
23	n-hexyloxy	-17.6 56.9(α) 16.69(β) 8.80(γ) 5.08(δ) 2.57( ) 1.67 (ε)	RT	Benzene	11
24	cyclohexy-loxy	-18.3[a] 122.0(α) 19.0(β) 17.3(ε) 10.2(γ) 9.8(δ) 7.5(ε)	30	Benzene	11
25	cholester-yloxy	-17.7[a,b]	30	Benzene	11

[a] extrapolated from spectrum reported in ref. 11

[b] See ref. 11 for substituent proton resonances

isotropic shifts in the remaining members of the series was effected by assuming that the pseudocontact shifts are all proportional to the corresponding geometry factors. Agreement between the calculated shifts and a_i values was fair, and, in general, the contact shifts were less than 50 ppm. For the ring protons an average geometry factor of $-7.97 \times 10^{-22}\,cm^{-3}$ was used to calculate a pseudocontact shift of 19.1 ppm and a contact shift of -28 ppm. While this contact shift is similar in magnitude to that calculated for the alkoxy compounds, the calculated pseudocontact shifts for the two series are opposite in sign. This implies that the replacement of -OR by -R caused a reversal of sign in the magnetic anisotropy term of eq. 3 (i.e., $\chi_{\parallel}-\chi_{\perp}$).

Recently, Amberger (13) has assigned the bands in the absorption spectrum of 3. In this analysis a set of first-order crystal field functions was derived which models the known temperature dependence of the magnetic susceptibility. From these parameters, the isotropic ^1H NMR shifts of the ring protons were factored into contact and pseudocontact components. Using the geometry factor of Marks ($-7.97 \times 10^{-22}\,cm^{-3}$) or that of Fischer ($-5.49 \times 10^{-22}\,cm^{-3}$) the calculated pseudocontact shifts at 25°C are 2.38 and 1.64 ppm and the calculated contact shifts are -11.58 and -10.84 ppm, respectively.

Interestingly, all of the calculated contact shifts for the ring protons in these Cp_3U-X compounds are of the same sign and of the same order of magnitude as the isotropic shift in Cp_4U, suggesting that the ring metal bonding in all of these compounds is quite similar. Replacement of one Cp in Cp_4U by any other ligand lowers the symmetry of the complex leading to magnetic anisotropy and pseudocontact contributions to the isotropic ^1H NMR shifts. Lower symmetry alone does not completely control the magnetic anisotropy. The substituent has a profound effect which can serve to change the sign of the magnetic anisotropy term in eq. 3 and hence, the sign of the pseudocontact shift.

The temperature dependence behavior of the ring proton isotropic shifts also reflects the effects of lower symmetry. While the ring proton shift in Cp_4U shows a linear dependence on T^{-1} from -106°C to 133°C, the ring proton shifts of Cp_3U-X compounds 2-5, 8-10, 12, 17-18, and 23-25 all show marked deviations from linearity. The alkyl-substituted systems show linear behavior from ca. -150°C to room temperature but deviate from linearity above room temperature. The alkoxy compounds show apparent linearity from ca. 200°C to 400°C but deviations from linearity below 200°C. All of the halides except for the fluoride display a slight curvature from 200°C to 400°C. The variable temperature behavior of the fluoride is solvent dependent and reflects the formation of dimers.

The presence of the paramagnetic center in Cp_3U-X compounds also serves as an internal shift reagent and as such has been used as a conformational probe. In a variable temperature ^1H NMR study, Marks and co-workers (30) have observed line broadening of

the borohydride proton resonances in 6. The broadening was not a result of temperature dependent changes in boron quadrupolar relaxation but instead was interpreted as indicative of slowing of the chemical exchange process between bridging and terminal protons. Estimation of the coalescence temperature as -140 ± 20°C leads to a calculated $\Delta G^{\neq}$ for the process of 5.0 ± 0.6 kcal mole^{-}. Similarly, the energy barrier to rotation of the isopropyl group in Cp_3U-i-C_3H_7 has been estimated to be E_a = 10.5 ± 0.5 kcal mole^{-1} from computer simulated line shape analysis of variable temperature spectra (12). From the coalescence temperature for fluxionality between monohapto- and trihapto-bonding of the allyl group in Cp_3U-allyl of 43°C, a value of 8.0 kcal mole^{-1} for $\Delta G^{\neq}$ for the process was calculated (12), while in cyclohexyloxy-UCp_3, a lower limit for $\Delta G^{\neq}$ for ring inversion of the cyclohexyl ring has been estimated to be 2.3 kcal mole^{-1} (11).

2. Uranocenes. Edelstein and co-workers (5) proposed that the ^1H isotropic shift in uranocene can be approximated by

$$\delta_{ISOTROPIC} = \frac{\chi_{||}-\chi_{\perp}}{3} \frac{3\cos^2\vartheta-1}{R^3} + \frac{Ai}{3} \frac{16 g_J' \beta e}{5kT} \qquad (5)$$

The pseudocontact term is simply the axially symmetric form of eq. 3. The contact term is eq. 2, where $\hat{S}$ and g_J have been evaluated using a crystal field model for bis-cyclooctatetraene-actinide sandwich compounds proposed by Karraker (31).

The ground state term for U^{+4} is $^3H_4$. In a crystal field of D_{8h} symmetry this ninefold degenerate state is split into four doublets (J_Z = ±4, ±3, ±2, ±1) and one singlet (J_Z = 0). Analysis of bulk magnetic susceptibility data led to selection of the ground state as J_Z = ±4, provided that an effective orbital reduction factor of k = 0.8 was included in the crystal field calculations to correct covalent contributions to metal ligand bonding (32). This model successfully predicts the magnetic behavior of uranocene, neptunocene, and plutonocene assuming: 1) only the lowest crystal field state is populated in the temperature range T << 400 K; 2) there is no mixing of J states by the crystal field; 3) the effects of intermediate coupling are small and can therefore be neglected (31).

A direct result of the J_Z = ±4 ground state is in the limit of kT << D, the total crystal field splitting, $\chi_{||} = 3\chi_{av}$ and $\chi_{\perp} = 0$ where

$$\chi_{av} = 1/3\ \chi_{||} + 2/3\ \chi_{\perp} \qquad (6)$$

Thus, the magnetic susceptibility component of the pseudocontact shift was evaluated from bulk susceptibility measurements. Using geometric data from the x-ray structure of Raymond and Zalkin (33) and a magnetic moment of 2.4 B.M., Edelstein and co-workers

calculated the pseudocontact shift for uranocene ring protons, (entry 1, Table II). These authors used the Curie Law to relate X and μ_{eff}, while the magnetic data obeyed the Curie-Weiss Law, with μ_{eff} = 2.4 B.M. and θ = 9.6°K. Neglect of the Weiss constant, (i.e., the Curie Law instead of the Curie-Weiss Law) underestimates the value of X_{av} resulting in smaller values for the pseudocontact shift. This underestimation amounts to about 3.5% for the ring ^1H resonances in uranocene (entry 2, Table II).

Since the calculated pseudocontact shifts are smaller in magnitude than the observed isotropic shift, Edelstein, et.al., concluded that an upfield contact component contributes to the total isotropic shift, indicative of covalency in the ligand metal bonds of uranocene.

TABLE II

Earlier Analyses of Isotropic ^1H Shifts of Uranocene

Proton	$3\cos^2\theta-1/R^3$ x 10^{21} cm^{-3}	Temp °C	μ_{eff} B.M.	Isotropic shift (ppm)	Pseudocontact shift (ppm)	Contact shift (ppm)
uranocene[a] ring	-3.55	29	2.4	-41.9	-14.0	-27.9
uranocene[b] ring	-3.55	29	2.4	-41.9	-14.5	-27.4
octamethyl[c] ring	-2.0	25	2.38	-41.3	-7.9	-33.4
octamethyl[c] ring	-5.9	25	2.38	-6.0	-23.6	+17.6
uranocene[c] ring	-2.0	25	2.38	-42.6	-7.9	-34.7

(a) Ref. 5. (b) Correction for Curie-Weiss Law; see text.
(c) Ref. 6.

The plot of shift vs T^{-1} was linear in accord with Curie-Weiss magnetic behavior and in agreement with the linearity predicted by eq. 5. The intercept, however, was ca. 7 ppm instead

of zero as predicted by eq. 5.

Subsequently, the ^1H NMR of 1,1',3,3',5,5',7,7'-octamethyluranocene was analyzed in a similar manner (6). The contact shifts for the ring and α-protons were found to be similar in magnitude, but opposite in sign, implying spin density in a π-MO, and transfer of spin density via a spin polarization type mechanism (entries 3 and 4 in Table II). In this paper, a new, significantly smaller, value for the pseudocontact shift in uranocene was reported (entry 5, Table II). This value was calculated using better geometric data from the refined x-ray structure of uranocene by Raymond and co-workers (34).

These results led to a simple model for the contact shifts in uranocenes shown in Fig. 2 (35). In the ground state, orbital angular momentum dominates so the two f-electrons on the metal have their magnetic moments opposed to the applied field. Electron density donated from filled ligand molecular orbitals to vacant metal orbitals will be spin-polarized so the net spin density in the ligand π-MO gives rise to a magnetic moment aligned with the applied field. Relay of spin density via a spin polarization mechanism affords an upfield shift to the ring protons, and via hyperconjugation, a downfield shift to the α-carbons. Subsequent spin transfer results in an alternating upfield, downfield shift pattern, which decreases substantially the greater the number of sigma bonds between the observed nucleus and the ring carbons.

Separation of the isotropic shifts in uranocenes into pseudocontact and contact components is certainly an appealing method of attributing covalent character to bonding in uranocene. However, Hayes and Thomas (7) have advised caution in making deductions about covalency from NMR data on actinide complexes. In these compounds J is assumed to be a good quantum number and thus, both spin and orbital angular momentum contribute to the observed magnetic moment. In actinide complexes, the spin magnetic moment may not be parallel to the net magnetic moment, which is aligned with the applied field. In fact, it is opposed if the 5f shell is less than half full as in uranocene. Hence, direct transfer of spin density to a ring proton will give rise to a downfield shift.

Second and more importantly, the ligand metal interaction in organometallic complexes involves only certain orbitals on both the ligand and the metal. The electronic states giving rise to shifts in an NMR experiment may not involve these orbitals. Hence, little if any direct information on covalency can be derived from NMR experiments. In general, one must consider the occupancy of the relevant orbitals in the crystal field states populated over the temperature range of the NMR experiment in attempted correlation of contact shifts with specific modes of bonding.

Nevertheless, a model with spin polarization of ligand electrons donated to empty metal orbitals gives rise to positive spin

density in the ligand system and the observed upfield shift to the ring protons. Such electron donation to metal orbitals does relate to bonding. Moreover, it appears that contact shifts do contribute to both the ring and α-proton isotropic shifts in uranocene and 1,1',3,3',5,5',7,7'-octamethyluranocene. Because both ring and α-positions experience contact and pseudocontact shifts it is impossible to test if the assumptions used in factoring the observed shifts are valid. Of particular interest are the assumptions concerning the magnetic anisotropy term ($\chi_{\parallel} - \chi_{\perp}$). Typically, contact shifts are effectively zero if at least three atoms (i.e., four sigma bonds) separate the observed nucleus from the paramagnetic center (15,35). Ideally, in a 1,1',3,3',5,5',7,7'-octaalkyluranocene, where the alkyl groups have β or γ protons, the observed isotropic shifts for these positions would be solely pseudocontact in nature. Unfortunately, none of these systems is known and attempts to prepare the t-butyl compound have not been successful (36).

Numerous substituted uranocenes are now known and could, in principle, provide useful tests. Other factors now, however, become involved and need to be evaluated. The lower symmetry of these compounds means that χ_x and χ_y are no longer constrained to be equal and the eq. 3 needs to be considered in its entirety. Moreover, the substituent could have an effect on magnetic anisotropy. Finally, some substituents have more than one possible conformation which would need to be considered.

If the magnetic moment of a paramagnetic molecule obeys the Curie or Curie-Weiss Law, variable temperature ^{1}H NMR can serve as a conformational probe. Conformationally rigid nuclei or those rapidly oscillating between conformations of equal energy, will exhibit a linear shift dependence on T^{-1} while those which undergo exchange between conformations differing in energy will show a non-linear dependence. Equation 3 shows that the slope of these plots will depend upon the sign of A_i and the sign of the geometry factor.

In the remainder of this paper we will present NMR results for a variety of uranocenes as a function of temperature. The results will be analyzed in terms of the component contact and pseudo-contact contributions with due regard to the foregoing considerations.

II. The Variable Temperature ^{1}H NMR of Uranocene and Substituted Uranocenes

In this section we summarize the experimental results for a number of substituted uranocenes. The compounds studied are listed in Table III and Fig. 3.

The spectra were run on the Berkeley 180 MHz FT NMR spectrometer equipped with a variable temperature probe. All spectra were run in toluene-d_8. In general, spectra were taken at 10° intervals from at least the range -80°C to 70°C. The temperature

TABLE III

Uranocenes Analyzed by Variable Temperature ^1H NMR

26	Uranocene
27	1,1'-Dimethyl-
28	1,1'-Diethyl-
29	1,1'-Di-n-butyl-
30	1,1'-Diisopropyl
31	1,1'-Dineopentyl-
32	Mono-t-butyl
33	1,1'-Di-t-butyl
34	1,1',4,4'-Tetra-t-butyl-
35	1,1',3,3',5,5',7,7'-Octamethyl-
36	1,1'-Diphenyl-
37	1,1'-Bis(p-dimethylaminophenyl)-
38	Dicyclobuteno-
39	Dicyclopenteno-
40	Bis(dimethylcyclopenteno)-
41	1,1'-Di(t-butoxycarbonyl)-
42	Mono-(t-butoxycarbonyl)-
43	1,1'-Di(1,3,5,7-cyclooctatetraenyl)-

of the probe was monitored by a pre-calibrated thermocouple 5 mm from the sample tube, and could be held to ±0.3°C over the dynamic temperature range. Shifts were measured relative to the methyl group of toluene rather than stopcock grease; the latter shifted ca. 0.2 ppm over the temperature range. The shifts are reported relative to TMS by assigning the toluene methyl resonance as 2.09 ppm. This resonance differs from that in protiotoluene (2.31 ppm). Often this resonance is erroneously assigned the same value as in the protio-compound; however, we have experimentally verified the difference which is a recognized secondary deuterium isotope effect in ^1H NMR spectroscopy (37,38).

A. Diamagnetic Reference Compounds. Analysis of the isotropic shifts requires referencing the observed shifts to their positions in the spectrum of a corresponding hypothetical diamagnetic uranocene. The diamagnetic thorocenes are probably the closest analogy to such a model uranocene and several of these compounds have now been reported (39,40). The difference between

the ^1H resonances in the thorocenes and the corresponding cyclooctatetraene dianions is small (Table IV); hence, without important error isotropic shifts in all of the uranocenes discussed in this chapter can be referenced to the ^1H shifts in the corresponding cyclooctatetraene dianions. For those cyclooctatetraenes where the dianion has not been isolated and characterized by ^1H NMR, the shifts have been estimated by comparison with other cyclooctatetraene dianions. The error resulting from such reference is probably no more than 1-2 ppm.

TABLE IV

The ^1H NMR Resonances of Cyclooctatetraene Dianions and Thorocenes in THF (ref. 39, 40)

	δ ppm from TMS ring	substituent		
COT[a]	5.9			
thorocene	6.5			
n-butylCOT[a]	5.7	2.9	1.3	0.9
1,1'-di-n-butylthorocene	6.5	3.2	1.6	1.0
methylCOT[a]	5.6	2.8		
1,1'-dimethylthorocene	6.5	3.1		
t-butylCOT[a]	5.7	1.5		
1,1'-di-t-butylthorocene	6.5	1.7		

[a] as the dipotassium salt

B. The Temperature Dependent ^1H NMR of Uranocene and Octamethyluranocene. Our initial interest was in verifying the temperature dependence of the ^1H isotropic shift in uranocene and the reported non-zero intercept at $T^{-1}=0$. Recent laser Raman studies by Spiro and co-workers (41) have established that the first excited state in uranocene is 466 cm^{-1} above the ground state. Thus, the isotropic shift may not vary linearly with the inverse of the temperature from -100°C to 100°C. Indeed, below 100°K some controversy exists concerning the temperature dependence of the magnetic moment in uranocene (42,43).

The temperature dependence of the isotropic shift in uranocene was measured on two independent samples from -80°C to 100°C. At the same nominal temperature slight differences in the shift between the two samples are undoubtedly due to slight differences in the true temperature of the samples and provide an estimate of the error in temperature measurement or measurement of the resonance frequency in this study.

The plot of shift vs T^{-1} (fig. 4, Table V) is strictly linear with an extrapolated intercept at $T^{-1}=0$ of zero within experiment-

al error. The difference between this result and that reported by Edelstein et al. (5), appears to arise entirely from uncertainty in measurement of the temperature. In the earlier work the uncertainty in the temperature at both the high and low extremes was +3.0°C while in this study it is +0.3°C. In fact, if one takes into account the reported error in the temperature measurements in the earlier work, the data can be fitted with a straight line which intercepts zero at $T^{-1}=0$. (Fig. 5).

TABLE V

Least Squares Linear Regression Analysis of VT ^{1}H NMR Data for Ring Protons in Uranocene, Octamethyluranocene and the Unsubstituted Ring in Monosubstituted Uranocenes.

Compound	Slope	Intercept	r^2
26, Uranocene Run #1	-12.83±0.07	-0.32±0.32	0.9992
Uranocene Run #2	-12.94±0.06	0.21±0.21	0.9997
Uranocene (ref.6)	-14.70±0.17	6.96±0.64	0.9991
32, Mono-t-butyl[a]	-12.62±0.04	-0.32±0.19	0.9998
41, Mono-t-butoxy-carbonyl[a]	-13.54±0.12	1.88±0.47	0.9989
35, Octamethyl	-13.12±0.03	2.45±0.14	0.9999

(a) Unsubstituted ring; the substituted ring data are in Table IX.

Octamethyluranocene, 35, has effective 4-fold symmetry and χ_x and χ_y are constrained to be equal on the nmr time scale. The temperature dependence of the ring protons of this compound is compared with uranocene in Fig. 6 and Table V. The non-zero intercept is probably due to referencing the isotropic shift to the tetramethylCOT dianion; note in Table IV that the ring protons of dimethylthorocene differ from methylCOT dianion by almost 1 ppm.

The near-identity of the slopes of the lines in Fig. 6 has important implications. The geometry factor for the ring protons of octamethyluranocene is essentially identical to that for uranocene itself; hence, according to eq. 5, any significant change in $\chi_\perp$ would be expected to produce a significant change in slope. The fact that methyl substitutents have little effect on the slope means either that $\chi_\perp$ does not change significantly by methyl substitution or that the effect of a change in $\chi_\perp$ is almost exactly balanced by an opposing change in the contact shift.

C. Monosubstituted Uranocenes. Some monosubstituted uranocenes are known, compounds with one COT and one substituted COT ligands. The mono-t-butoxycarbonyluranocene, 42, was prepared by reaction of one mole of the corresponding COT dianion with one mole of COT dianion itself and UCl_4(44). It could be separated from the disubstituted compound, 41, also formed, by its greater stability towards hydrolysis. Mono-t-butyluranocene, 32, was obtained and measured as a 1.8:1 mixture with the disubstituted compound, 33. A separate preparation of pure 33 allowed complete analysis of the mixture. Mono-(di-t-butylphosphino)uranocene has also been reported by Fischer, et al(45).

The importance of these compounds for nmr interpretations is that we can look at the unsubstituted ring in systems where χ_x and χ_y are not constrained by symmetry to be equal. In both of the monosubstituted uranocenes investigated, the proton resonance of the unsubstituted ring is a singlet.

At 30°C, the protons of the unsubstituted ring in mono-t-butyluranocene resonate at 0.51 ppm lower field and those in the mono-ester resonate at 0.43 ppm higher field than the ring protons in uranocene. These differences are small but real and were established independently by observing the spectrum of mixtures of these compounds.

The temperature dependence of the unsubstituted ring proton resonances are linear functions of T^{-1} and the slopes of shift vs. T^{-1} are identical within experimental error to that of uranocene (fig. 7, Table V). The slight difference in intercepts at $T^{-1}=0$ undoubtedly result from using the proton resonance of cyclooctatetraene dianion as a diamagnetic reference for all the compounds.

Changes in the linewidths at half heights of the unsubstituted ring resonances as a function of temperature parallels that of uranocene and results from the known change in paramagnetic relaxation times as a function of temperature rather than the onset of coalescence (Table VI) (19). This implies that ring rotation in monosubstituted uranocenes is rapid on the NMR time scale or that rotation is slow and the differences between the resonance frequency of the non-equivalent protons is smaller than the linewidths of the observed signals. Bis(1,4-di-t-butylcyclooctatetraene)-uranium, 34, does show coalescence of all of the proton resonances at low temperature corresponding to a barrier to rotation of 8.4 kcal mol^{-1}(46). Substituents smaller than t-butyl should show smaller barriers. We conclude that uranocene and the monosubstituted uranocenes are freely rotating on the nmr scale at our temperatures.

For complete rotation, the final term in eq. 3 averages to zero; hence, if $\frac{1}{2}(\chi_x + \chi_y)$ differs seriously from $\chi_\perp$ of uranocene, we would expect a significant change in slope. The near constancy of the observed slopes for all of the unsubstituted rings together with the ring protons of 35 provides highly suggestive, albeit not rigorous, evidence that $\chi_x = \chi_y = \chi_\perp$ for all of these compounds. These approximations certainly make a strong

TABLE VI

Linewidth at Half Height of ^1H NMR Resonances of Uranocene (H_z)

	-70°C	30°C	70°C
26, uranocene	102	90	76
32, mono-t-butyl[a]	45	33	30
41, mono-t-butoxycarbonyl-	50	38	32

(a) Unsubstituted ring.

working hypothesis.

Recently, Fischer (15,45) has independently arrived at the same conclusion based on the temperature dependence behavior of the ^1H NMR resonances of the two monosubstituted uranocenes, $(C_8H_8)(C_8H_7R)U$, $R = P(t\text{-}C_4H_9)_2$ and $Sn(t\text{-}C_4H_9)_3$. In both of these compounds the unsubstituted ring resonances is reported to be identical with that in uranocene.

D. Magnetic Susceptibility of Substituted Uranocenes. We examine further implications of the potential effects of substituents on magnetic anisotropy. In the limit of rapid ring rotation the final term in eq. 3 averages to zero; in the limit of frozen rotations this term can contribute and result in non-linearity. The ^1H NMR data on 34 provide a test (46). At temperatures above coalescence the rings are freely rotating and the three pairs of equivalent ring protons on each ring are linear functions of T^{-1}. Below coalescence the three ring proton resonances split into six and all six resonances are again linear functions of T^{-1}. Moreover, the average of appropriate pairs of resonances is close to the value extrapolated from three resonances above coalescenece. Thus, even in the "frozen rotation" region, the last term in eq. 3 makes little contribution, a result that implies $\chi_x = \chi_y$.

We conclude that substitution of the uranocene skeleton, although formally lowering the symmetry of the complex, exerts only a small perturbation on the crystal field around the uranium. The magnetic behavior remains primarily an atomic property and from the point of view of the uranium atom, it still experiences a C_{8v} crystal field as in uranocene. Thus, to a good first approximation, substituted uranocenes can be viewed as having effective axial symmetry regardless of the rate of ring rotation.

We next inquire whether this result is consistent with other physical properties of uranocenes. Bulk magnetic susceptibility measurements at low temperature on several substituted uranocenes appear to suggest that within experimental error the magnetic properties of all uranocenes are essentially identical and equal

to 2.4±0.2 B.M. (Table VII). This result is consistent with the idea confirmed by X_α Scattered Wave (47) and Extended Hückel MO (48) calculations that the magnetic properties of uranocenes are determined principally by the two unpaired electrons that are primarily metal electrons.

E. ^{1}H NMR of Substituted Uranocenes. Table VIII summarizes the chemical shifts relative to TMS for a number of uranocenes at a common temperature (30°C). The results are summarized for ring and substituent protons for convenience.

F. The Temperature Dependence of Proton Resonances in Substituted Uranocenes. In substituted cyclooctatetraene dianions where substitution lifts the symmetry imposed equivalency of the ring protons, the difference in resonance frequency of the magnetically non-equivalent protons is sufficiently small that the observed resonances appear as a broadened singlet even in high field NMR experiments. Likewise in corresponding substituted thorocenes, the non-equivalent ring proton resonances appear as a broadened signal with no assignable features. However, in substituted uranocenes the non-equivalent ring proton resonances all appear as well resolved singlets for all of the uranocenes whose ^{1}H NMR has been reported.

The structure of a sufficient number of substituted uranocenes has been determined by single crystal X-ray diffraction to establish that both the uranium-ring distance and the C_{ring}-C_{ring} bond distance are invariant, within experimental error, regardless of substituents on the uranocene skeleton. Assuming that the geometry factor for all of the ring protons is the same, and if $X_x = X_y$ as shown above, then the pseudocontact shift for each will be the same and the observed differences in resonance frequency must arise from differences in the contact shift at the magnetically non-equivalent ring positions. For comparison, differences in the isotropic shifts of the non-equivalent ring protons in substituted bisarenechromium complexes have been attributed to differences in the contact shift (52).

For purposes of convenient identification, the ring proton resonances in the NMR of substituted uranocenes will be labeled alphabetically starting with the lowest field resonance. This does not imply that the "A" resonancees in two different uranocenes correspond to the same ring position. We shall discuss below the assignment of the individual ring proton resonances.

The temperature dependence of the ring proton resonances of the uranocenes listed in Table III were determined and plotted as shifts vs. T^{-1}. In all, 60 individual ring proton resonances in 17 different uranocenes were observed. In all cases except for one position in dicyclobutenouranocene, 38, the shifts are linear functions of T^{-1} from at least the range -70°C to 70°C. The non-linearity of the 3-position in dicyclobutenouranocene, 38, probably reflects a temperature dependent geometry change of the ring

TABLE VII

Magnetic Properties of Uranocenes

	Substituent[a]	Temp. Range °K	μ_{eff} B.M.	Weiss Constant °K	Ref.
26	H	4.2-4.5	2.43	9.56	42
	H	4-10	3.33	9.4	31
	H	10-42	2.3	0.9	31
	H	12-72	2.42	2.9	43
	H	180-300	2.62	3	43
	H	10-300	2.6		5
27	CH_3	14.5-81.5	2.26±0.2	17	49
28	CH_2CH_3	3-8	2.86	14.9	31
	CH_2CH_3	10-27	1.9	0.4	31
	CH_2CH_3	14.7-79.6	2.13±0.2	-7	49
29	$(CH_2)_3CH_3$	3-10	2.85	5.8	31
	$(CH_2)_3CH_3$	10-50	2.3	2.6	31
36	C_6H_5	14-100	2.65±0.2	12.2±3	50
38	cyclobuteno	15-100	2.35±0.2	8.5	14
39	cyclopenteno	15-95.6	2.4±0.2	16.1	49
44	cyclohexeno	14.4-97.8	2.65±0.2	23	49
35	1,3,5,7-tetramethyl	1.9-73.7	2.2±0.2	11.3±3	50
	1,3,5,7-tetraphenyl	4.2-100	2.5±0.1	6.7±1	50
41	CO_2-t-C_4H_9	30-100	2.64±0.2	10.4	44

(a) Both rings substituted

TABLE VIII

^{1}H NMR Resonances of Substituted Uranocenes

δ ppm from TMS

	Substituent[a]	Shift[b] at 30°C
26,	H	-36.63
35,	1,3,5,7-tetramethyl	-35.15, -4.21 (CH_3)
27,	CH_3	-31.70, -33.67 (H5), -36.10,-40.39 -7.20 (CH_3)
28,	CH_2CH_3	-32.89, -34.45 (H5), -36.33, -39.7 -17.47 (CH_2), -1.20 (CH_3)
30,	i-C_3H_7	-35.50, -35.98, -36.00 (H5), -36.40 -14.47 (CH), -9.89(CH_3,d,J=4.4 Hz)
29,	n-C_4H_9	-32.64, -34.10 (H5), -36.22, -39.74 -19.03 (α-CH_2), 0.22 (β-CH_2) 0.98 (q-CH_2,m), 0.36 (CH_3,t,J= 6.3 Hz)
33,	t-C_4H_9	-33.43, -33.80, -37.30, -40.54 (H5) -11.49 (CH_3)
32,	t-C_4H_9	-33.41, -34.74, -39.51, -43.37 (H5) -36.02 (8H, unsubstituted ring), -10.82 (CH_3)
34,	1,4-di-t-butyl	-25.23, -39.66, -42.23 -10.25 (CH_3)
31,	neo-C_5H_{11}	-32.84, -33.42 (H5), -36.26, -41.07 -23.97 (CH_2), 3.86 (CH_3)
	$(CH_2)_3N(CH_3)_2$[d]	-31.5, -32.9 (H5), -34.9, -38.1, -18.3 (α-CH_2,t,J=7.5 Hz) 0.63 (β-CH_2,m), 113 (CH_3) 2.80 (γ-CH_2,t,J=7.0 Hz)
36,	C_6H_5	-34.29, -36.15, -36.45, -37.13 (H5) 0.76 (p,d,J=7.2 Hz) 0.85 (m,t,J=7.6 Hz) -13.95 (o,d,J=7.3 Hz)
37,	p-$(CH_3)_2NC_6H_4$	-34.29, -36.15, -36.46, -37.13 (H5) -14.10 (o,d,J=7.6 Hz) o.13 (m,d,J=7.6 Hz), -0.04 (CH_3)
38,	cyclobuteno	-27.70, -35.90, -43.80 -26.75 (α_{endo}) 19.65 (α_{exo}) (J=9.64 Hz)

TABLE VIII (cont.)

	Substituent[a]	Shift[b] at 30°C
39,	cyclopenteno	-32.12, -34.20, -41.15 -32.58 (β_{endo},m) -8.28 (β_{exo},m) -18.78 (α_{endo},m) 24.43 (α_{exo},m)
40,	dimethyl cyclopenteno	-32.43, -33.26, -39.83 -12.91 (CH_{3endo}) 5.39 (CH_{3exo}) -22.90 (α_{endo}) 8.28 (α_{exo}) (J=14.5 Hz)
44,	cyclohexeno	-30.64, -32.53, -38.70 -22.35 (β_{endo},m) -2.94 (β_{exo},m) -16.42 (α_{endo},m) 6.56 (α_{exo},m)
	$C(C_6H_5)_3$[e]	-21.35, -34.87, -49.50, -52.01(H5) 4.88 (o,d,J=6.8 Hz) 4.95 (m,t,J=6.6 Hz) 5.44 (p,t,J=6.6 Hz)
	OCH_3[d]	-27.5, -30.2 (H5), -35.6, -43.7 -3.73 (CH_3)
	O-t-C_4H_9[d]	-28.1, -28.7 (H5), -36.2, -45.7 2.08 (CH_3)
	$OCH_2CH\ CH_2$[d]	-27.9, -30.5 (H5), -35.5, -43.5 -0.33 (α-CH_2,d,J=5.0 Hz) 0.70 (trans-H, d,J=17.5 Hz) 1.75 (β-CH,m), 2.60 (cis-H,d,J=10.5 Hz)
41,	CO_2-t-C_4H_9	-30.51, -32.65, -36.01 (H5),-42.45 -6.07 (CH_3)
42,	CO_2-t-C_4H_9[c]	-29.42, -33.69, -36.0 (H5), -40.06 -37.06 (8H, unsubstituted ring) -6.27 (CH_3)
	$CO_2CH_2C_6H_5$	-29.81, -32.08, -36.23 (H5),-43.16 -2.98 (CH_2), -0.56 (o) 4.09 (m) 5.20 (p)
	$CO_2CH_2C_6H_5$[c]	-28.51, -32.40, -32.98 (H5),-40.63 -2.99 (CH_2), -36.06 (8H, unsubstituted ring) -1.16 (o) 3.94 (m) 5.30 (p)

TABLE VIII (cont.)

Substituent[a]	Shift[b] at 30°C
$CO_2CH_2CH_3$	-29.93, -32.69, -35.78 (H5), -42.14 -6.05 (CH_3), -4.23 (CH_2)
$CO_2CH_2CH_3$[c]	-28.84, -32.93, -36.14 (H5), -40.27 -6.57 (CH_3), -4.45 (CH_2), -37.07 (8H, unsubstituted ring)

(a) Substituent on each 8-membered ring.

(b) In monosubstituted cyclooctatetraene ligands the ring H5 could be identified by integration relative to the other ring proton resonances.

(c) Monosubstituted.

(d) Data from ref. 51 at 39°C.

(e) At 26°.

proton resulting from conformational changes in this strained ring system and will not be discussed further.

Some typical examples of the linear behavior found is summarized in Figs. 8-11. The complete set of plots is given in ref. 53 and the linear regressions are summarized in Table IX.

Note in these results that the total difference between the highest and lowest field resonance of the non-equivalent ring protons in all of the uranocenes increases as the temperature decreases. Moreover, the relative pattern of the ring proton resonances in each uranocene remains constant as a function of temperature except for the two phenyl-substituted uranocenes and 1,1'-biscyclooctatetraenyluranocene. In these latter cases the substituent ^1H NMR spectra show slowing of rotation and coalescence phenomena to be discussed below; these phenomena may also affect some of the ring protons.

The high degree of linearity in the temperature dependence of the ring proton shifts is evident from the correlation coefficients of the least squares regression lines (Table IX). The slopes of the lines are all negative and similar in magnitude to that of uranocene. However, the standard deviations of the extrapolated intercepts at $T^{-1}=0$ indicate that a number of the intercepts are non-zero. Ideally, eq. 3 predicts that all of the intercepts should be zero at $T^{-1}=0$.

Considering all of the ring proton resonances together, there is no apparent correlation between the non-zero intercepts and the magnitude of the isotropic shifts at a given temperature, say 30°C. However, for some individual uranocenes, it appears that a correlation does exist such that the intercept increases the larger the isotropic shift at a given temperature. This seems to

TABLE IX

Least Squares Linear Regression Lines For

Alkyl Uranocene Ring Proton Data

Fig. no.	Substitutent	Proton Resonance	Slope	Intercept	r^2
8	methyl	A	-10.89±0.05	-1.35±0.19	0.9997
		B	-11.20±0.05	-2.30±0.18	0.9997
		C	-12.80±0.06	0.57±0.24	0.9996
		D	-15.59±0.09	5.48±0.36	0.9994
9	t-butyl[a]	A	-12.12±0.04	0.75±0.17	0.9998
		B	-12.08±0.04	0.71±0.16	0.9998
		C	-14.03±0.04	0.92±0.17	0.9999
		D	-15.22±0.05	1.00±0.18	0.9999
10	t-butyl	A	-11.80±0.03	-0.37±0.12	0.9999
		B	-11.89±0.05	-0.51±0.18	0.9998
		C	-14.24±0.08	3.77±0.32	0.9995
		D	-15.59±0.11	4.96±0.41	0.9993
	ethyl	A	-10.95±0.06	-2.43±0.20	0.9994
		B	-10.85±0.06	-4.31±0.20	0.9994
		C	-13.12±0.08	1.17±0.31	0.9991
		D	-16.04±0.13	7.25±0.46	0.9986
	n-butyl	A	-10.78±0.02	-2.77±0.08	0.9999
		B	-10.73±0.02	-4.37±0.08	0.9999
		C	-12.85±0.03	0.39±0.11	0.9999
		D	-15.69±0.07	6.14±0.25	0.9996
	neopentyl	A	-11.27±0.05	-1.68±0.17	0.9998
		B	-11.15±0.05	-2.68±0.19	0.9997
		C	-13.01±0.05	0.58±0.19	0.9998
		D	-15.93±0.07	5.31±0.25	0.9998
	isopropyl	A	-13.06±0.05	1.68±0.19	0.9999
		B	-12.79±0.05	0.39±0.19	0.9998
		C	-13.12±0.05	1.40±0.19	0.9998
		D	-13.44±0.08	2.04±0.30	0.9995
	cyclobuteno	A	non-linear		
		B	-12.81±0.12	0.65±0.48	0.9984
		C	-17.58±0.20	8.45±0.77	0.9979
	cyclopenteno	A	-11.07±0.25	-1.50±1.02	0.9912
		B	-13.20±0.08	3.67±0.31	0.9994
		C	-16.84±0.23	9.02±1.04	0.9960
	dimethylcyclo-cyclopenteno	A	-10.29±0.05	-4.11±0.21	0.9996
		B	-12.26±0.06	1.52±0.22	0.9997
		C	-16.84±0.11	9.93±0.45	0.9993

TABLE IX (cont.)

Fig.no.	Substituent	Proton Resonance	Slope	Intercept	r^2
11	phenyl	A	-12.04±0.08	-0.71±0.32	0.9992
		B	-12.03±0.10	-2.58±0.38	0.9989
		C	-13.95±0.09	3.41±0.34	0.9994
		D	-12.05±0.10	-3.52±0.40	0.9988
	p-dimethyl-	A	-11.23±0.10	-3.49±0.41	0.9985
	aminophenyl-	B	-12.20±0.13	-0.49±0.53	0.9979
		C	-11.17±0.09	-5.21±0.38	0.9987
		D	-14.93±0.19	5.74±0.76	0.9971
	t-butoxy-	A	-11.02±0.08	0.19±0.31	0.9993
	carbonyl[a]	B	-12.47±0.12	2.89±0.47	0.9987
		C	-13.01±0.08	1.30±0.31	0.9995
		D	-14.62±0.09	0.19±0.36	0.9994
	t-butoxy-	A	-4.63±0.02	1.16±0.08	0.9997
	carbonyl	B	-10.52±0.07	-0.37±0.29	0.9993
		C	-12.60±0.12	2.36±0.47	0.9987
		D	-14.05±0.11	0.73±0.43	0.9991

[a]substituted ring of monosubsituted uranocene

suggest that the non-zero intercepts are in some way associated with the contact shift.

The linear dependence of the isotropic shifts on T^{-1} over the observed temperature range can imply one of two things: 1) both the contact and pseudocontact shifts are linear functions of T^{-1}; 2) the contact shift is a linear function of T^{-1} while the pseudocontact shift is a function of both T^{-1} and higher orders of T^{-1}, where the combined contact and pseudocontact T^{-1} dependence is large relative to the higher order terms of the pseudocontact shift. In principle, these two possibilites can be differentiated by observing the temperature dependence of α and β protons whose geometry factor is invarient with temperature. The contact shift for α and particularly for β-protons should be substantially smaller than for ring protons. Hence, their temperature dependence should be linear in T^{-1} if the former is true, but non-linear if the latter is true.

In fact, studies of a number of substituent protons in substituted uranocenes provide linear correlations with T^{-1} (54). The temperature dependence of the substituent proton resonances in 1,1',3,3',5,5',7,7'-octamethyl-, 35, mono-t-butyl-, 32, and 1,1'-di-t-butyluranocene, 33, are all linear. Similarly, both the methylene and methyl protons of 1,1'-dineopentyluranocene 31 are linear. For this case, the results imply a relatively fixed conformation with the t-butyl group swung away from the central uranium (conformation A in Figure 12; R=t-OBu). The non-linearity of

the methyl protons of 1,1'-diethyluranocene 28 is interpreted as an effect of temperature on the populations of different conformations having different pseudo-contact shifts. Conformation A in Figure 12 ($R=CH_3$) predominates but other conformations also contribute. We have no simple interpretation of the non-linearity of 1,1'-dimethyluranocene, 27, at this time. Some of the results are summarized in Table X.

An interesting special case is that of 1,1'-di(cycloocta-tetraenyl)uranocene, 43. Both Miller (55) and, recently, Spiegel and Fischer (56) have reported that the number of substituent and ring proton resonances vary as a function of temperature indicative of a dynamic process which is slow on the NMR time scale. Above 90°C, the spectrum consists of four ring proton resonances in an area ratio of 2:2:2:1 similar to that of other 1,1'-disubstituted uranocenes. At 30°C, six broad ring proton resonances are present and determination of relative areas is extremely difficult. Initially, we had hoped that monitoring coalescence of the ring protons in this system would provide a method of assigning individual ring proton resonances. However, interpretation of the temperature dependent changes was not straightforward and no assignment could be made.

Initially, the B ring resonance begins to broaden at 80°C, followed by the A resonance at ca. 70°C, and both merge into a single peak at 50°C. Below this temperature, they rapidly separate into three broad peaks at 40°C and to at least six peaks at 30°C. At 40°C, the C resonance also begins to coalesce followed by the D resonance at ca. 30°C. Below 30°C, it is not clear which of the peaks in the 'low temperature' spectrum are associated with peaks in the 'high temperature' spectrum. From 0°C to -80°C, eleven ring proton resonances are discernible; however, relative peak areas indicate that not all of the individual resonances are resolved.

Similar temperature dependence behavior is observed for the substitutent proton resonances. At 90°C, all of the resonances have coalesced into the baseline, while at 80°C a resonance appears at 1.8 ppm, followed at 70°C by the appearance of two broad resonances at -9.0 ppm and -14.9 ppm and a sharper resonance at ca. 0.0 ppm. Labeling these resonances as K (1.8 ppm), L (0.0 ppm), M (-9.0 ppm) and N (-14.9 ppm), the L resonance separates into two peaks at ca. 50°C, while the other resonances remain fairly sharp. At 30°C, the N resonance begins to broaden and separates into two peaks at 20°C, followed by broadening of the M resonance. At 10°C, the M and N regions each consist of two resonances while the two resonacnes of the L region are broadened. The behavior of the K resonance is obscured by the TMS/grease signal. At 0°C, the L region consists of four resonances. At -80°C, the M and N signals are both well separated sets of two resonances each while the K and L regions consist, respectively, of four and five sets of double resonances of essentially equal area.

TABLE X

Least Squares Regression Data for Alkyl Uranocene Substituent Proton Data vs T^{-1}

Compound	Proton Resonance	Slope	Intercept	r^2
α-Protons				
27	methyl	non-linear		
35	octamethyl	-5.53±0.04	11.19±0.14	0.9993
28	ethyl	-12.65±0.17	21.84±0.61	0.9962
29	n-butyl	-12.22±0.10	18.10±0.37	0.9995
31	neopentyl	-12.5 ± 0.73	14.02±0.28	0.9995
30	isopropyl	-8.58±0.05	11.47±0.20	0.9994
β-Protons				
32	mono-t-butyl	-5.42±0.03	4.42±0.10	0.9996
33	t-butyl	-5.60±0.07	5.32±0.25	0.9979
34	tetra-t-butyl	-5.09±0.06	5.03±0.22	0.9980
29	n-butyl	non-linear		
28	ethyl	non-linear		
30	isopropyl	-4.69±0.04	4.51±0.14	0.9991
γ and δ Protons				
31	neopentyl t-butyl	1.14±0.01	-0.97±0.03	0.9992
29	n-butyl $-CH_2$	non-linear		
29	n-butyl CH_3	non-linear		

Of the substituent resonances, only the M and N signals can be definitely assigned to the α position of the uncomplexed ring. At low temperature, the α position protons are equally distributed in four magnetically different environments.

A combination of slowing or effective stopping of several dynamic exchange processes could give rise to the observed changes in the spectrum: 1) tub-tub interconversion of the uncomplexed cyclooctatetraene ring; 2) double bond reorganization in the uncomplexed cycloocatetraene ring; 3) rotation about the C_{ring}-C_{α} bond; 4) ring-ring rotation in the uranocene moiety. The presence of four different α position resonances in the 'low temperature' spectrum requires that double bond reorganization be slow relative to the NMR time scale. This implies that in the 'high temperature' spectra, where double bond reorganization is rapid, four rather than seven substituent resonances should be observed. Unfortunately, due to solvent and instrumental limitations, we could not obtain spectra above 100°C to confirm this. The data do not permit further differentiation between the other possible dynamic exchange processes.

III. Identification of Ring Proton Resonances in Substituted Uranocenes.

In all of the mono- and 1,1'-disubstituted uranocenes prepared to date, the ^1H NMR resonances of the non-equivalent protons in the substituted rings are all well resolved singlets, three of area 2 and one of area 1. From Table VIII the total difference between the highest and lowest field resonances at 30°C in such uranocenes varies from 0.9 ppm to 30.6 ppm. It seems likely in most cases that the difference in ring proton resonances arises from differences in the contact shift at each of the non-equivalent positions in the 8-membered ring. One might therefore expect a correlation between the contact shift and the spin density at the various ring positions. Attempting such correlation requires assigning all of the ring proton resonances in 1,1'-disubstituted uranocenes.

Integration readily differentiates the 5 position, of area 1, from the remaining three postions, of area 2. Inspection of Table VIII shows that there is no apparent correlation between the electron-donating or withdrawing character of the substituent and the position of the 5 proton resonance relative to the other proton resonances. Figure 13 shows the patterns of ring proton resonances for some 1,1'-disubstituted uranocenes in a more schematic form. The pattern of the results strongly suggests that for primary alkyl substituents the assignments of the A,B,C, and D resonances are all the same. In all of these cases the B resonance is identified with the 5-position. Important changes do occur, however, for isopropyl and t-butyl substituents. For isopropyl, the ring proton resonances are closely bunched together.

For t-butyl, the 5-position is now the D-resonance for both the mono- or disubstituted uranocenes.

A tentative assignment of the other ring protons in the t-butylCOT ligand may be made in the following way. The barrier to rotation in tetra-t-butyluranocene, 34, suggests that conformations of 1,1'-di-t-butyluranocene with the t-butyl rings close (Figure 14a) will be relatively unpopulated compared to populations with the bulky t-butyl groups farther apart, Figure 14b, c, and d. Next, we note that the substituted ring protons in mono-t-butyluranocene, 32, show some significant differences from 1,1'-di-t-butyluranocene, 33. The $\Delta\sigma$ values for the A,B,C, and D resonances are, respectively, -0.02, 0.94, 2.21, 2.83 (H5) ppm. The largest change is associated with the known position H5 for which conformation (d) in Figure 14 has a high population. This suggests that the presence nearby of a t-butyl group in the other ring has a perturbing effect to shift the ring proton resonance to lower field. On this basis, H2, which rarely has such a "deshielding" perturbation, may be assigned resonance A. Similarly, conformation (c) in Fig. 14 is probably more highly populated than (b); hence, H4 is assigned to resonance C and H3 to B. That is, this argument provides assignments of resonances A,B,C, and D to positions 2,3,4, and 5, respectively. Although Figure 14 is based on eclipsed conformations the same approach applies to analogous staggered conformations.

This approach finds confirmation in the effect of the t-butyl group of one ring on the unsubstituted ring of mono-t-butyl-uranocene, 32. In this compound, each hydrogen is equally likely to have a t-butyl group nearby in the other ring. The result is an average shift of 0.6 ppm having the appropriate direction and approximate magnitude.

A more rigorous approach to assigning resonances to structure is by deuterium labeling. Methylcyclooctatetraene-4-d was prepared via sulfone chemistry pioneered by Pacquette and co-workers (57), (Fig. 15). Lewis acid catalyzed addition of SO_2 to COT gave the sulfone which was dilithiated with butyllithium and quenched with D_2O. The dideuterio compound was mono-metallated with butyllithium and quenched witn methyl iodide. Attempted prior alkylation followed by introduction of deuterium was found to be far less successful. Pyrolysis of the deuteriosulfone by slow sublimation through a pyrex tube packed with glass helices at 400° gave the desired methylcyclooctatetraene-4-d in 87% yield. Reduction to the dianion with potassium metal and reaction with UCl_4 gave 1,1'-dimethyluranocene-4,4'-d_2. The nmr spectrum showed incorporation of 1.5d. Only the A resonance was affected and can be rigorously assigned the 4-position.

We also prepared deuterated butylcyclooctatetraenes by bromination of butylcyclooctatetraene followed by dehydrobromination, metallation with butyllithium and quenching with D_2O. Location of the deuterium in the product is, however, not straightforward. Pacquette has studied the bromination of methylcyclooctatetraene

and has identified different bromination products on different occasions (58,59). It appears from his work that bromination-dehydrobromination of methylcyclooctatetraene can lead to all four possible methylbromocyclooctatetraenes.

In our case with the butyl compound, various workup procedures were applied to the butylbromoCOT product; e.g., reduced pressure short path distillation in one run, silica gel chromatography in another. The deuterio-products were converted to the corresponding deuterated 1,1'-dibutyluranocenes giving the nmr results in Table XI. Included are the total deuterium incorporations by mass spectral analysis. The A resonance is identified by analogy to dimethyluranocene (vide supra) as the 4-position. The

TABLE XI

Proton NMR of Deuterated 1,1'-Dibutyluranocenes

Run	Total d-incorporation	% Deuterium Incorporation in Ring Resonances			
		A	B	C	D
1	1.59	69	20	0	0
2	0.93	28	5	20	0
3[a]	1.74	61	0	14	0

(a) Prepared earlier with somewhat different conditions by Dr. C. LeVanda.

B resonance is established by integration to be the 5-position. Of the two remaining positions only the D resonance is undeuterated in all preparations. It seems most likely by consideration of steric hindrance effects in the reaction mechanism for dehydrobromination that the undeuterated position must be the 2-position. Accordingly, the most probable assignment of the ring resonances in primary alkyl uranocenes is that A, B, C, D correspond to positions 4, 5, 3, 2, respectively. The corresponding $\Delta\delta$ in dimethyluranocene relative to uranocene itself is, therefore, 2, -3.8 ppm; 3, +0.5 ppm; 4, +4.9 ppm; 5, 3.0 ppm. Only the 2-position, adjacent to the alkyl group, suffers an upfield shift.

Some comparisons suggest that these effects may be additive. For example, in octamethyluranocene, 35, a given ring proton is 1,2 with respect to two methyls and 1,4 with respect to two more. An additive effect would give $\Delta\delta$=2 (-3.8) + 2 (4.9)=2.2 ppm. The actual $\Delta\delta$ relative to uranocene is 1.5 ppm (Table VIII) in good agreement. Further development of this approach may prove useful in other assignments. For example, if the $\Delta\delta$ values for 1,1'-di-ethyluranocene (-3.1, +0.3, 3.7, 2,2 for the 2,3,4,5 positions, respectively) are applied to the three ring positions of bis-cyclohexenouranocene, 44, we can assign the ring resonances A, B, C to positions 5,4,3, respectively, and obtain the following

experimental and calculated $\Delta\delta$ ppm, respectively, relative to uranocene: 3-, -2.1, -2.8; 4-, +4.1, +4.0; 5-, +6.0, +5.9.

These correspondences help confirm the assignments made above. But now we can inquire why the 2-position in primary alkyl uranocenes is furthest upfield whereas in t-butyluranocene it is furthest downfield. This marked difference suggests a significant difference in structure. In all uranocenes whose structures have been established by X-ray analysis so far, ring-carbon substituent bonds are tilted towards the central uranium by several degrees. This effect probably occurs to provide better overlap between ligand π and central metal orbitals. With the t-butyl group, however, even for a ring-carbon bond coplanar with the ring, methyl hydrogens approach within van der Waals distance of the other ring. We suggest, therefore, that in t-butyluranocenes the t-butyl group is tilted away from the uranium with a consequent perturbation of the C_8 ring that shows up in the nmr spectra. We hope to test this prediction by X-ray structure analysis of suitable compounds.

IV. Factoring the ^{1}H Isotropic Shifts in Alkyluranocenes.

The discussions above have shown that the pseudocontact component of the isotropic shift in 1,1'-dialkyluranocenes is accurately given by the axially symmetric form of eq. 3 and thus, these systems can be used in evaluating both the assumptions employed in deriving, and the value of the anisotropy term $(\chi_{\parallel} - \chi_{\perp})$ used, by previous workers in factoring isotropic shifts in uranocenes. In this section we present such an analysis comparing pseudocontact shifts calculated assuming $\chi_{\parallel} - \chi_{\perp} = 3\chi_{av}$ and assuming values of $\chi_{\parallel} - \chi_{\perp}$ derived from isotropic shift and geometric data for protons which experience little or no contact shift. However, prior to such analysis it is important to be cognizant of the accuracy of calculated pseudocontact and contact shifts. Irrespective of the method or the equation(s) used to calculate pseudocontact shifts, three factors limit their accuracy: a) errors in measurement of the isotropic shift; b) errors in the assumed geometry; c) errors in the magnetic anisotropy. For uranocenes, the uncertainty associated with the isotropic shifts is small, larger for the assumed geometries and largest for the assumed anisotropy difference. In calculating shifts assuming $\chi_{\parallel} - \chi_{\perp} = 3\chi_{av}$, Table VII shows that to a good first approximation, $\chi_{av} = 2.4 \pm 0.2$ B.M. for all uranocenes. As a result of the 10% uncertainty in this value, calculated pseudocontact shifts will have an uncertainty of at least 10%. Similarly, in using a value of $\chi_{\parallel} - \chi_{\perp}$ derived from isotropic shift and geometric data, the uncertainty associated with calculated pseudocontact shifts will depend upon the reference compound chosen and will undoubtedly be of the same order of magnitude. Thus, the factored shifts in the following section will have an error of at least 10%.

In the following discussion, all calculated shifts are derived assuming a temperature of 30°C. For numerical convenience, the anisotropy term $\chi_{\parallel} - \chi_{\perp}$ will be expressed in terms of $\mu_{\parallel}^2 - \mu_{\perp}^2$.

Fischer has proposed useful and important methods for factoring the isotropic shifts of uranocenes into contact and pseudo-contact components (15); values were reported for uranocene, 1,-1',3,3',5,5',7,7'-octamethyluranocene, and 1 1'-bis(trimethylsilyl)uranocene using a non-zero value of $\chi_{\perp}$. Fischer arrived at values of $\mu_{\parallel}^2$ and $\mu_{\perp}^2$ at several temperatures from the ratio of the geometry factor and the isotropic shift for methyl protons in bis(trimethylsilyl)-uranocene, and bulk magnetic susceptibility data, assuming no contact contributions to the isotropic shift of the methyl protons. From the published data of Fischer, the value of $\mu_{\parallel}^2 - \mu_{\perp}^2$ at 30°C is 8.78 BM^2.

His results show that $\mu_{\perp}$ is small but not zero. The non-zero $\mu_{\perp}$ component has the effect of reducing the magnitude of pseudo-contact shifts. There seems little doubt that Fischer's result is qualitatively correct but the several assumptions required, especially of geometry, make them quantitatively suspect. For example, 1,1'-bis(trimethylsilyl)uranocene shows the same pattern of ring proton resonances as 1,1'-di-t-butyluranocene; hence, the structure may involve a trimethylsilyl group bent away from the ring plane. Such a distortion would change the calculated geometry factors and the derived value of $\mu_{\parallel}^2 - \mu_{\perp}^2$.

In our approach we have determined $\mu_{\parallel}^2 - \mu_{\perp}^2$ by another approach involving dicyclobutenouranocene, 38, and have compared the results for 1,1'-di-t-butyluranocene, 33, and 1,1'-dineo-pentyluranocene, 31. These three test systems contain α, β and γ-protons constrained in relatively known geometric configurations relative to the uranium center. In the latter two compounds, contact contributions to the t-butyl isotropic shift must be vanishingly small, whereas in the first compound, the fixed geometric relationship of the methylene group relative to the 8-membered ring suggests that both hyperconjugation and the contact shift must be effectively the same for the exo and endo protons, if the contact shift results from hyperconjugation transfer of spin density.

The average geometry factor of the t-butyl group in 1,1'-di-t-butyluranocene was taken as 1/6 (A + 2C + 2E + G) (Fig. 12, R=CH_3) in Table XII and for the t-butyl group in the neopentyl substitutent it was taken as conformation A (Fig. 12, R=t-Bu) (Table XIII). While the methylene protons in dicyclobutenouranocene are conformationally mobile, as evidenced by their temperature dependent ^1H NMR spectra, we assume that their average position in solution is given adequately by the average position of the methylene groups in the X-ray crystal structure. Although atomic coordinates are reported for all of the atoms in the X-ray structure, geometry factors calculated from these data are probably in error for two reasons: 1) the reported coordinates are not thermally corrected, and thus, they reflect an average

Cring - Cring bond length of 1.39 A rather than a thermally corrected value of 1.41 A; 2) the two reported $H_{exo} - C_{\alpha} - H_{endo}$ bond angles of 104° and 106° are certainly too small and reflect the large uncertainty associated with the location of hydrogen atoms by X-ray diffraction.

TABLE XII

Calculated Geometry Factors $\frac{3\cos^2\theta-1}{R^3}$

For β Methyl Group
($R=CH_3$ in Fig. 12)

Conformation[a]	Planar Gi x $10^{21}cm^{-3}$	5° Tip[b] Gi x $19^{21}cm^{-3}$
A	2.563	1.793
B	1.756	0.9977
C	-0.7736	-1.557
D	-5.081	-6.082
E	-10.32	-11.83
F	-14.64	-16.65
G	-16.45	-18.74

(a) Figure 12.

(b) Towards uranium.

Formally, the fused 4-membered ring is similar to the 4-membered ring of cyclobutene or benzocyclobutene, and the methylene bond angle should be similar to the methylene bond angle in these compounds. Gas phase electron diffraction of cyclobutene gives this angle as 110° (60), whereas J_{13C-H} coupling constants yield a value of 114° (61). Similarly, J_{13C-H} coupling constant analysis predicts a bond angle of 112° in benzocyclobutene (62). Thus, 112° is certainly a more realistic value for the $H_{exo} - C_{\alpha} - H_{endo}$ bond angle. In calculating geometry factors for the exo and endo protons, we have used the idealized geometry in Fig. 16, which more accurately describes the location of the methylene protons, rather than the coordinates of the atoms from the published X-ray crystal structure. The geometry factors for the exo and endo protons calculated with these data are -0.7097×10^{21} cm^{-3} and -16.97×10^{21} cm^{-1}, respectively.

Considering first the Edelstein, et al. (5), proposal that $\chi_{\parallel} - \chi_{\perp} = 3\chi_{av}$, the average μ_{eff} of 2.4 ± 0.2 B.M. for uranocene $_2$ and substituted uranocenes affords a value of 17.28 BM^2 for μ_{av}. The calculated pseudocontact shifts for a t-butyl group and the t-butyl protons in a neopentyl group, assuming coplanarity of the

C_{ring}-C_α bond and the 8-membered ring, are -23.7 ppm and 14.3 ppm, respectively. With a tipped substituent the values are, respectively, -28.8 ppm and 6.35 ppm. Comparison with the experimental isotropic shifts of -13.29 ppm and 2.76 ppm shows that the calculated values overestimate the magnitude of the pseudocontact shift. Factoring the isotropic shifts of the methylene protons in the cyclobuteno group further reinforces this result. The calculated pseudocontact shifts are: exo -2.80 ppm, endo -67.0 ppm. By difference from the experimental isotropic shifts of 15.19 ppm (exo) and -31.20 ppm (endo), the corresponding contact shifts are 18.0 ppm (exo) and 35.8 ppm (endo). The large difference in the contact shifts cannot result from slight differences in hyperconjugation, which may arise from the ca. 6° decrease in the 180° dihedral angle between the 4- and 8-membered rings, but clearly results from overestimation of the pseudocontact shift.

Reducing the magnitude of the calculated pseudocontact shifts requires smaller values of the anisotropy term $\chi_{||} - \chi_{\perp}$, which can only result if $\chi_{\perp} \neq 0$. This result provides independent confirmation of the same result of Fischer cited above. We noted also that both the electronic structure of uranocene proposed by Warren (63), assuming a $J_z = \pm 4$ ground state, and a recent model proposed by Fischer (15), assuming a $J_z = 3$ ground state, show that $\chi_{\perp}$ is non-zero, and less than $\chi_{||}$, at 30°C.

Using Fischer's value of $\mu_{||}^2 - \mu_{\perp}^2 = 3.78$ BM^2 the calculated pseudocontact shifts for the t-butyl groups in 1,1'-di-t-butyl- and 1,1'-dineopentyl uranocene are -12.1 ppm and 7.28 ppm, respectively, for coplanar substituents, and -14.6 ppm and 3.22 ppm, respectively, for tipped substituents. Agreement between the calculated pseudocontact shifts and the observed isotropic shifts is rather good. Calculation of the pseudocontact shifts for the cyclobuteno substituent, however, gives values of -1.42 ppm (exo) and -34.0 ppm (endo) with corresponding contact shifts of 16.6 ppm (exo) and 2.80 (endo). Again the difference in contact shifts for the two positions is too large to be theoretically justifiable. It can not arise from the difference between the reported atomic coordinates from the X-ray crystal structure data and our 'idealized' geometry for cyclobutenouranocene. The calculated pseudocontact shifts using geometry factors derived from the average position of the methylene groups in the X-ray structure are -2.36 ppm (exo) and -28.5 ppm (endo), with corresponding contact shifts of 17.5 ppm (exo) and -2.7 ppm (endo). Moreover, increasing the dihedral angle between the fused rings in the cyclobuteno ligand from 173° to 180° results in a larger discrepancy between the calculated contact shifts for the two positions.

The value of the contact shift for the exo and endo protons can be derived indirectly from the calculated contact shift for the methyl groups in 1,1'-dimethyluranocene. Assuming a geometry factor for the methyl group (Table XIV) as 1/6(A + 2C + 2E + G) (R = H in Fig. 12) and $\mu_{||}^2 - \mu_{\perp}^2 = 8.78$ BM^2, the calculated pseudocontact shifts for the coplanar and tipped substituent are

-11.8 ppm and -12.8 ppm, respectively. From the experimental isotropic shift of -10.00 ppm, the corresponding contact shifts are 1.8 ppm and 2.8 ppm. Contact shifts for α-protons are assumed to arise from hyperconjugative transfer of spin. Hyperconjugation between a carbon p orbital and a carbon-hydrogen bond is a function of the dihedral angle between the two. When unpaired spin is transferred by hyperconjugation, the magnitude of both the hyperfine coupling constant in ESR, and the contact shift in NMR, can be expressed by

$$B = B_o \cos^2(\phi) \qquad (7)$$

where ϕ is the dihedral angle and B_o is the magnitude of the hyperfine coupling constant or the contact shift when $\phi=0$ (64-67). Evaluation of B_o from the contact shift for the methyl group affords values of 3.54 ppm and 5.54 ppm, respectively, for a planar and a tipped substituent.

The fixed orbital angle between the p-orbitals of the 8-membered ring and the methylene C-H bonds in the cyclobuteno substituent permit evaluation of the contact shift for the exo and endo protons from B_o. In our idealized structure of the ligand, the dihedral angle is 25° which compares favorably with the average

TABLE XIV

Calculated Geometry Factors $\frac{3\cos^2\theta-1}{R^3}$

For α Protons
(R = H in Fig. 12)

Conformation[a]	Planar Gi x 10^{21} cm^{-3}	5° Tip[b] Gi x 10^{21} cm^{-3}
A	1.388	0.3599
B	0.6717	-0.3653
C	-1.503	-2.604
D	-5.053	-6.357
E	-9.424	-11.14
F	-13.23	-15.46
G	-14.76	-15.55

(a) Figure 12.
(b) Toward Uranium

value of 22° from the X-ray data. With $\phi=25°$, the calculated contact shift is 2.91 ppm when $B_o=3.54$ ppm and 4.5 ppm when $B_o=5.54$ ppm. These values are significantly different from those obtained by difference from the isotropic shifts for the exo and endo protons and the calculated pseudocontact shifts assuming $\mu_{||}^2 - \mu_{\perp}^2 = 8.78$ BM^2. The discrepancy between the calculated contact shifts for the exo and endo protons in 1,1'-dicyclobutenouranocene using Fischer's value of $\mu_{||}^2 - \mu_{\perp}^2$ can only arise from

underestimation of the pseudocontact shifts resulting from underestimation of $\mu_{||}^2 - \mu_{\perp}^2$.

The known geometry of the methylene protons in the cyclobuteno permits an independent calculation of $\mu_{||}^2 - \mu_{\perp}^2$. Assuming that the contact shift for both methylene protons is equla, the relationship between $\chi_{||} - \chi_{\perp}$, the isotropic shift, δ, and the geometry factor G for the exo and endo protons is given by

$$\frac{\chi_{||} - \chi_{\perp}}{3} = \frac{\delta_{exo} - \delta_{endo}}{G_{exo} - G_{endo}} \qquad (8)$$

This equation leads to a value of 12.5 BM^2 for $\mu_{||}^2 - \mu_{\perp}^2$ with corresponding pseudocontact shifts of -2.03 (exo), -48.5 ppm (endo) and a contact shift of 17.2 ppm.

This value of $\mu_{||}^2 - \mu_{\perp}^2$ yields respective pseudocontact shifts of -17.2 ppm and 10.4 ppm for the t-butyl groups in 1,1'-di-t-butyl- and 1,1'-dineopentyluranocene, assuming coplanar substituents, and -20.8 ppm and 4.59 ppm, assuming tipped substituents. Although agreement between the calculated and experimental shifts for the neopentyl t-butyl group, assuming a tipped substituent is good, agreement between the t-butyl calculated and experimental data is poor for the coplanar and worse for the tipped substituent. If we assume that the difference in the observed and the calculated shifts for the t-butyl substituent is contact in nature, neither its sign nor its magnitude are consistent with the predicted sign based on transfer of spin by spin polarization, or the magnitude limits established from analysis of the temperature dependence of the methyl resonance in 1,1'-diethyluranocene. Thus, if the difference in calculated and observed shift does not arise from the anisotropy term, it must result from inaccuracies in the assumed geometry factor.

We can now return to our conclusion in the last section where we deduced from the pattern of ring proton resonances and from steric considerations that t-butyl substituents in uranocenes must be tilted away from uranium. This argument does not apply to the neopentyl group which is a normal primary alkyl substituent for which the ring-CH_2 bond can be tilted towards uranium without difficulty.

Tipping the substituent away from the uranium center leads to better agreement between the calculated and observed shift for the t-butyl group in 1,1'-di-t-butyluranocene. With $\mu_{||}^2 - \mu_{\perp}^2 = 12.5$ BM^2, a tip of 5° away from uranium affords a calculated pseudocontact shift of -13.7 ppm, in excellent agreement with the experimental isotropic shift of -13.29 ppm.

To further demonstrate the difficulties associated with selecting an appropriate reference compound from which $\mu_{||}^2 - \mu_{\perp}^2$ can be derived, we shall derive $\mu_{||}^2 - \mu_{\perp}^2$ from the geometry factor and the isotropic shift of the t-butyl group in 1,1'-dineopentyluranocene. Our conformational analysis showed that the substi-

tuent is locked in conformation A in Fig. 12. For a coplanar substituent, the derived value of $\mu_{||}^2 - \mu_{\perp}^2$ is 3.33 BM^2, while tipping the substituent 5° toward the uranium leads to a value of 7.51 BM^2. However, relaxing the restriction of exclusive population of conformation A, and assuming an extremely small population of any other conformation where the geometry factor and the pseudocontact shift are negative, will greatly increase the derived value of $\mu_{||}^2 - \mu_{\perp}^2$.

Thus, evaluation of the geometry factor is extremely important in deriving a value of $\mu_{||}^2 - \mu_{\perp}^2$ from geometric and isotropic shift data. Two factors favor our approach to deriving a value of $\mu_{||}^2 - \mu_{\perp}^2$ from the methylene protons in dicyclobutenouranocene: 1) the single crystal X-ray data and the variable temperature ^{1}H NMR data provide an excellent estimate for the geometry factors for the two methylene protons; 2) calculation involves using the isotropic shift and geometry factor of two magnetically non-equivalent protons rather than one.

From the contact shift of the exo and endo protons in dicyclobutenouranocene, derived using $\mu_{||}^2 - \mu_{\perp}^2 = 12.5$ BM^2, a value of B_o, the maximum contact shift for an α-proton, can be calculated from eq. 7. Taking ϕ=25° leads to a value of 20.9 ppm for B_o.

Assuming a geometry factor of 1/6 (A + 2B + 2D + C) for the methyl group in 1,1'-dimethyluranocene, the calculated pseudocontact shifts are -16.8 ppm and -18.2 ppm, respectively, for a coplanar and a tipped substituent. By difference from the isotropic shift, the contact shifts are 6.76 ppm and 8.17 ppm, while calculation of the contact shift from B_o affords a value of 8.71 ppm. Agreement between the contact shifts calculated by both methods is excellent, particularly for the tipped substituent.

Considering the α-protons in 1,1'-dineopentyluranocene, if A is the only populated conformation of the neopentyl substituent, then the conformation of the α-protons is EE (Fig. 12). The calculated pseudocontact shift is -26.9 ppm (coplanar), -31.8 (tipped) and by difference from the experimental isotropic shift of -23.97 ppm, the contact shifts are 2.93 ppm (coplanar), and 7.83 ppm (tipped). Calculation of the contact shift from B_o affords a value of 5.23 ppm.

Comparison of the calculated pseudocontact shifts for the neopentyl t-butyl resonances with the isotropic shift showed that the tipped geometry affords better agreement between the two values, but still the value of calculated shift was approximately twice that of the experimental isotropic shift. However, an extremely small population of any conformation other than A will readily decrease the magnitude of the calculated pseudocontact shift for the t-butyl resonance. Assuming an extremely small population of conformations other than A, how does this affect the factored shifts of the α-protons?

From the geometry factors in Table XIV and eq. 7, the pseudocontact shift for any conformation other than EE will be less negative than that for EE, while the contact shift will be

smallest in magnitude for EE and larger for any other conformation. The magnitude of these changes is such that the isotropic shift will be less negative as the population of conformations other than EE increase. Thus, assuming a tipped substituent and an extremely small population of conformations other than A for the neopentyl substituent in 1,1'-dineopentyluranocene, leads to better agreement between the calculated pseudocontact and contact shifts for both the α and t-butyl resonance, than assuming either exclusive population of conformation A or a coplanar substituent.

This analysis also accounts for the observed trend in the isotropic shifts of the α-protons in 1,1'-diethyl-, 1,1'-di-n-butyl-, and 1,1'-dineopentyluranocene, respectively, -17.47 ppm, -19.03 ppm, and -23.97 ppm. The increase in magnitude of the isotropic shift directly parallels the increasing stability of the preferred conformation of the substituent, (i.e., conformation A in Figure 12).

V. Summary.

Previous attempts at factoring the isotropic ^{1}H NMR shifts in uranocene and substituted uranocenes have assumed that these systems can be viewed as having effective axial symmetry. The temperature dependent ^{1}H NMR spectra of uranocene and a variety of substituted uranocenes clearly verify this assumption and show that eq. 9 can be used to evaluate the pseudocontact contribution to the total isotropic shift in uranocenes. In this equation $\chi_x \cong \chi_y$ for substituted uranocenes and are replaced by $\chi_\perp$.

$$\delta_{PSEUDOCONTACT} = \frac{\chi_{||} - \chi_\perp}{3N} \quad \frac{3\cos^2\theta - 1}{R^3} \qquad (9)$$

Early attempts to factor the isotropic shifts in alkyl-uranocenes using eq. 9 were not completely successful because of failure to correctly assess the conformation of the substituent in solution and overestimation of the value of the anisotropy term $\chi_{||} - \chi_\perp$ (5,6,14).

In alkyl-substituted uranocenes, our conformational analysis shows that a primary alkyl substituent populates principally conformations in which the dihedral angle between the substituent $C_\alpha - C_\beta$ bond and the ring plane is close to 90° on the side of the ring away from the metal. X-ray structure analyses have shown generally that substituents have ring-C_α bonds tilted several degrees towards uranium. The pattern of ring proton resonances and steric considerations suggest that t-butyl and related substituents are tilted away from uranium.

Another important result of this study is the confirmation of Fischer's demonstration that $\chi_\perp$ is not equal to zero in uranocene. Early attempts to factor isotropic shifts in uranocene have generally assumed that $\chi_\perp = 0$, and leads to overestimation of

the anisotropy term. A precise value of $\chi_\perp$ is difficult to determine rigorously from analysis of available NMR data. We have found that $\mu_\parallel^2 - \mu_\perp^2 = 12.5$ BM^2 leads to the best internal consistency factored isotropic shifts for a wide variety of 1,1'-dialkyluranocenes. Assuming $\mu_{av}^2 = 5.76$ BM^2 and $\mu_\parallel^2 - \mu_\perp^2 = 12.5$ BM^2, at 30°C, the corresponding values of $\mu_\parallel^2$ and $\mu_\perp^2$ are 14.09 and 1.59 BM^2, respectively. This implies that $\chi_\parallel/\chi_\perp \cong 8$ in uranocene, a value substantilly larger than Fischer's ratio of $\chi_\parallel/\chi_\perp \cong 2.8$ (15).

As a result of $\chi_\perp \neq 0$, early work on factoring the isotropic shift of the ring protons in uranocene underestimated the magnitude of the contact shift. Using our value of $\mu_\parallel^2 - \mu_\perp^2 = 12.5$ BM^2, the pseudocontact and contact shifts for uranocene ring protons are -8.30 ppm and -34.2 ppm, ($G_i = -2.34 \times 10^{21}$ cm^{-3}), respectively. Thus, this study confirms that both contact and pseudocontact interactions contribute to the observed isotropic shifts in uranocenes. The contact component is dominant for ring protons, but rapidly attenuates with increasing number of σ-bonds between the observed nucleus and the uranium such that the contact shift is effectively zero for β-protons.

The value of the contact shift for ring protons in uranocene is of the same sign but about 10 to 15 ppm larger in magnitude than the contact shift for ring protons in CP_3U-X compounds. If a direct correlation exists between the magnitude of the contact shift and the degree of covalency in ligand-metal bonding in these systems, then the NMR data suggest a higher degree of covalency in the ligand-metal bonds in uranocene.

Acknowledgement

This research was supported in part by the Division of Nuclear Sciences, Office of Basic Energy Sciences, U.S. Department of Energy under contract no. W-7405-Eng-48. We are indebted to Dr. Norman Edelstein and Professor R.D. Fischer for valuable discussions and suggestions.

Literature Cited

1. von Ammon, R.; Kanellakopulos, B.; Fischer, R.D. Chem. Phy. Let., 1968, 2, 513.

2. Siddall, T.H. III; Stewart, W.E.; Karraker, D.G. Chem. Phy. Let., 1969, 3, 498.

3. von Ammon, R.; Kanellakopulos, B.; Fischer, R.D.; Laubereau, R. Inorg. Nucl. Chem. Let., 1969, 5, 219.

4. von Ammon, R.; Kanellakopulos, B.; Fischer, R.D. Chem. Phy. Let., 1970, 4, 553.

5. Edelstein, N.; La Mar, G.N.; Mares, F.; Streitwieser, A. Jr. Chem. Phy. Let., 1971, 8, 399.

6. Streitwieser, A. Jr.; Dempf, D.; La Mar, G.N.; Karraker, D.G.; Edelstein, N. J. Am. Chem. Soc., 1971, 93, 7343.

7. Hayes, R.G.: Thomas, J.L. Organomet. Chem. Rev. A., 1971, 7, 1.

8. Paladino, N.; Lugli, G.; Pedretti, U.; Brunelli, M.; Giacometti, G. Chem. Phy. Let., 1970, 5, 15.

9. Brunelli, M.; Lugli, G.; Giacometti, G. J. Mag. Res., 1973, 9, 247.

10. Fischer, R.D.; von Ammon, R.; Kanellakopolus, B. J. Organomet. Chem., 1970, 25, 123.

11. von Ammon, R.; Fischer, R.D.; Kanellakopolus, B. Chem. Ber., 1972, 45, 105.

12. Marks, T.J.; Seyam, A.M.; Kolb, J.R. J. Am. Chem. Soc., 1973, 95, 5529.

13. Amberger, H.D. J. Organomet. Chem., 1976, 116, 219.

14. Berryhill, S.R. Ph.D. Thesis, UC Berkeley, 1978.

15. Fischer, R.D. in "Organometallics of the f-Elements"; Marks, T.J.; Fischer, R.D., Eds.; D. Reidel Pub. Co., Boston, Mass.; 1979; p 337.

16. Eaton, D.R.; Phillips, W.D. "Advances in Magnetic Resonance"; Waugh, J.S. Ed.; Academic Press, New York, N.Y.; 1965; vol.1, p 119.

17. "NMR of Paramagnetic Molecules: Principals and Applications"; La Mar, G.N.; Horrocks, W. DeW. Jr.; Holm, R.H., Eds.; Academic Press, New York, N.Y.; 1973.

18. Webb, G.A. "Annual Reports on NMR Spectroscopy"; Mooney, E.F., Ed.; Academic Press, New York, N.Y.; 1970; vol. 3, p 211.

19. Webb, G.A. "Annual Reports on NMR Spectroscopy"; Mooney, E.F., Ed.; Academic Press, New York, N.Y.; 1975, vol. 6A, p 2.

20. Kurland, R.J.; McGarvey, R.B. J. Mag. Res., 1970, 2, 286.

21. Drago, R.S.; Zisk, J.I.; Richman, R.M.; Perry, W.D. J. Chem. Ed., 1974, 51, 371, 465.

22. McConnell, H.M.; Chestnut, D.B. J. Chem. Phys., 1958, 28, 107.

23. McConnell, H.M.; Robertson, R.E. J. Chem. Phys., 1958, 29, 1361.

24. Kluiber, R.W.; Horrocks, W. DeW. Jr. Inorg. Chem., 1967, 6, 166.

25. Horrocks, W. DeW. Jr. Inorg. Chem., 1970, 9, 690.

26. Horrocks, W. DeW. Jr.; Sipe, J.P. III Science, 1972, 177, 994.

27. von Ammon, R.; Kanellakopulos, B.; Fischer, R.D.; Laubreau, P. Inorg. Nucl. Chem. Let., 1969, 5, 315.

28. Sebala, A.E.; Tsutsu, M. Chem. Let., 1972, 775.

29. von Ammon, R.; Kanellakopulos, B.; Fischer, R.D. Radiochim. Acta., 1969, 11, 162.

30. Marks, T.J.; Kolb, J.R. J. Am. Chem. Soc., 1975, 97, 27.

31. Karraker, D.G. Inorg. Chem., 1973, 12, 1105.

32. Hayes, R.G.; Edelstein, N. J. Am. Chem. Soc., 1972, 94, 8688.

33. Zalkin, A.; Raymond, K.N. J. Am. Chem. Soc., 1969, 91, 5667.

34. Avdeef, A.; Raymond, K.N.; Hodgson, K.O.; Zalkin, A. Inorg. Chem., 1972, 11, 1083.

35. von Ammon, R.; Fischer, R.D. Ang. Chem. Int., 1972, 11, 675.

36. Miller, M.J.; Streitwieser, A. Jr. J. Org. Chem., submitted.

37. MacDonald, C.G.; Hannon, J.S.; Sternhell, S. Aust. J. Chem., 1964, 17, 38.

38. Batiz-Hernandez, H.; Bernheim, R.A. "Prog. in NMR Spectroscopy"; Emsley, J.W.; Feeney, J.; Sutcliffe, L.H., Eds.; Pergamon Press, New York, N.Y.; 1967; p 63.

39. Streitwieser, A. Jr. "Organometallics of the f-Elements";

Marks, T.J.; Fischer, R.D., Eds.; D. Reidel Pub. Co., Boston, Mass.; 1979; p 149.

40. Streitwieser, A. Jr.; LeVanda, C. Inorg. Chem., submitted.

41. Dallinger, R.F.; Stein, P.; Spiro, T.G. J. Am. Chem. Soc., 1978, 100, 7865.

42. Karraker, D.G.; Stone, J.A.; Jones, E.R. Jr.; Edelstein, N. J. Am. Chem. Soc., 1970, 92, 4841.

43. Amberger, H.D.; Fischer, R.D.; Kanellakopolus, B. Theoret. Chim. Acta., 1975, 37, 105.

44. Streitwieser, A. Jr.; Burgherd,H.P.C.; Morrell, D.G.; Luke, W.D. Inorg. Chem., submitted.

45. Fischer, R.D.; Spiegl, A.W.; Dickert, F. personal communication.

46. Luke, W.D.; Streitwieser, A. Jr. to be published.

47. Rösch, N.; Streitwieser, A. Jr. J. Organomet. Chem., 1978, 145, 195.

48. Schilling, B. unpublished results.

49. Luke, W. unpublished results.

50. Edelstein, N.; Streitwieser, A. Jr.; Morrell, D.G.; Walker, R. Inorg. Chem., 1967, 15, 1397.

51. Harmon, C.A.; Bauer, D.P.; Berryhill, S.R.; Hagiwara, K.; Streitwieser, A. Jr. Inorg. Chem., 1977, 16, 2143.

52. Anderson, S.E.; Drago, R.S. Inorg. Chem., 1972, 11, 1564.

53. Luke, W.D. Dissertation; University of Calif., 1979.

54. Luke, W.D.; Berryhill, S.R.; Streitwieser, A. Jr. to be published.

55. Miller, M.J. unpublished results.

56. Spiegel, A.W.; Fischer, R.D. Chem. Ber., 1979, 112, 116.

57. Paquette, L.A.; Ley, W.V.; Meisinger, R.H.; Russell, R.K.; Oku, M. J. Am. Chem. Soc., 1974, 96, 5806.

58. Paquette, L.A.; James, D.R.; Birnberg, G. J. Am. Chem. Soc.,

1974, 96, 7454.

59. Paquette, L.A.; Henzel, K.A. J. Am. Chem. Soc., 1975, 97, 4649.

60. Bak, B.; Led, J.J.; Nygaard, L.; Rastrup-Anderson, J.; Sorensen, G.O. J. Mol. Struct., 1969, 3, 369.

61. Levy, G.C.; Nelson, G.C. "Carbon-13 Nuclear Magnetic Resonance for Organic Chemistr"; Wiley-Interscience, New York, N.Y.; 1972.

62. Gunther, H.; Jikeli, G.; Schmicker, H.; Prestien, J. Ang. Chem. Int. Ed., 1973, 12, 762.

63. Warren, K.D. "Structure and Bonding"; Springer-Verlag, New York, N.Y.; 1977, vol. 33, p 97.

64. Kron, R.; Weiss, A.; Polzner, H.; Bischer, E. J. Am. Chem. Soc., 1975, 97, 644.

65. Gerson, F.; Moxhuk, G.; Schwyzer, M. Hel. Chim. Acta., 1971, 54, 361.

66. Scroggins, W.T.; Rettig, M.F.; Ming, R.M. Inorg. Chem., 1976, 15, 1381.

67. Heller, C.; McConnell, H.M. J. Chem. Phys., 1960, 32, 1535.

Figure Captions

Fig. 1. Coordinates R_i, θ_i, and ψ_i of a nucleus i in the coordinate system x, y, z, with the three principal components χ_x, χ_y, χ_z of the magnetic susceptibility.

Fig. 2. Spin-polarization in uranocenes. Arrows shown refer to magnetic moments.

Fig. 3. Structures of compounds studied.

Fig. 4. Isotropic shift vs T^{-1} for uranocene.

Fig. 5. Comparison of older data (dot-dash line, ref. 5) with present results (dashed line).

Fig. 6. Isotropic shift vs T^{-1} for uranocene and the ring protons in 1,1',3,3',5,5',7,7'-octamethyluranocene, 35.

Fig. 7. Isotropic shift vs T^{-1} for uranocene and the ring protons in the unsubstituted ring of mono-t-butyl, 32, and mono-t-butoxycarbonyluranocene, 42.

Fig. 8. Isotropic shift vs T^{-1} for the ring protons in 1,1'-dimethyluranocene, 27.

Fig. 9. Isotropic shift vs T^{-1} for the ring protons in the substituted ring of mono-t-butyluranocene, 32.

Fig. 10. Isotropic shift vs T^{-1} for the ring protons in 1,1'-di-t-butyluranocene, 33.

Fig. 11. Isotropic shift vs T^{-1} for the ring protons in 1,1'-diphenyluranocene.

Fig. 12. Conformations of the substituent in substituted uranocenes shown in Newman projection form with the uranium atom below the plane of the ring in each figure.

Fig. 13. Pattern of ring proton resonances of 1,1'-dialkyluranocenes. H5 is indicated by its reduced intensity.

Fig. 14. Several conformations of 1,1'-disubstituted uranocenes about the central axis. The 1'-substituent is shown with the dotted line.

Fig. 15. Preparation of methylcyclooctatetraene-4-d.

Fig. 16. Assumed structure of cyclobutenouranocene, 38.

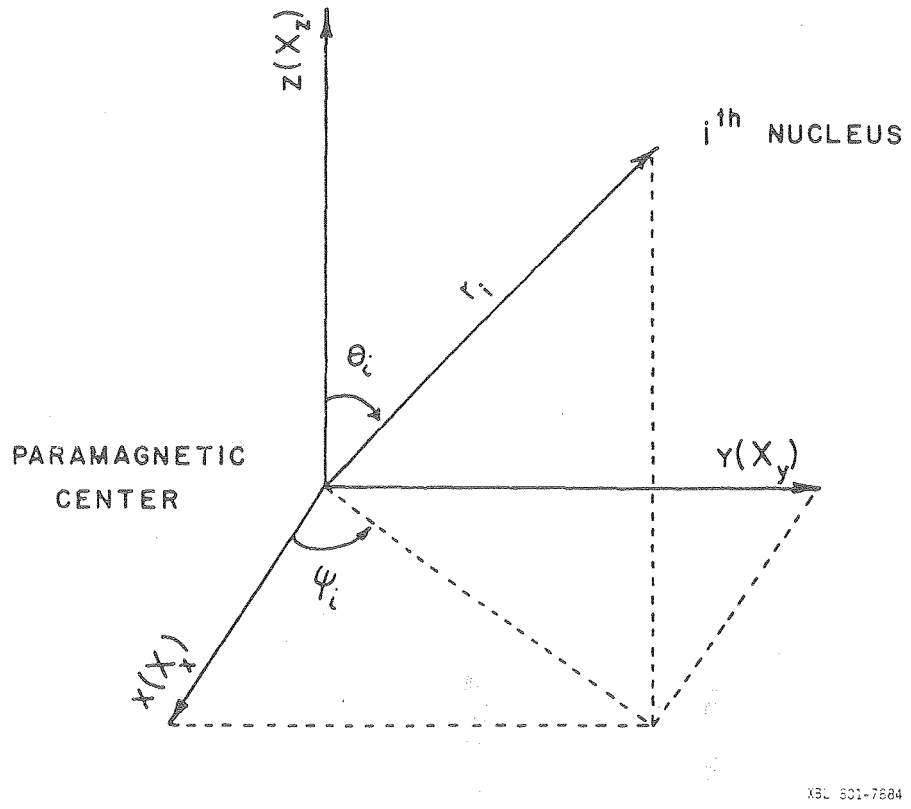
Z(X_z)
i^th NUCLEUS
r_i
θ_i
PARAMAGNETIC
CENTER
Y(X_y)
ψ_i
x(X_x)
XBL 831-7884

Figure 1

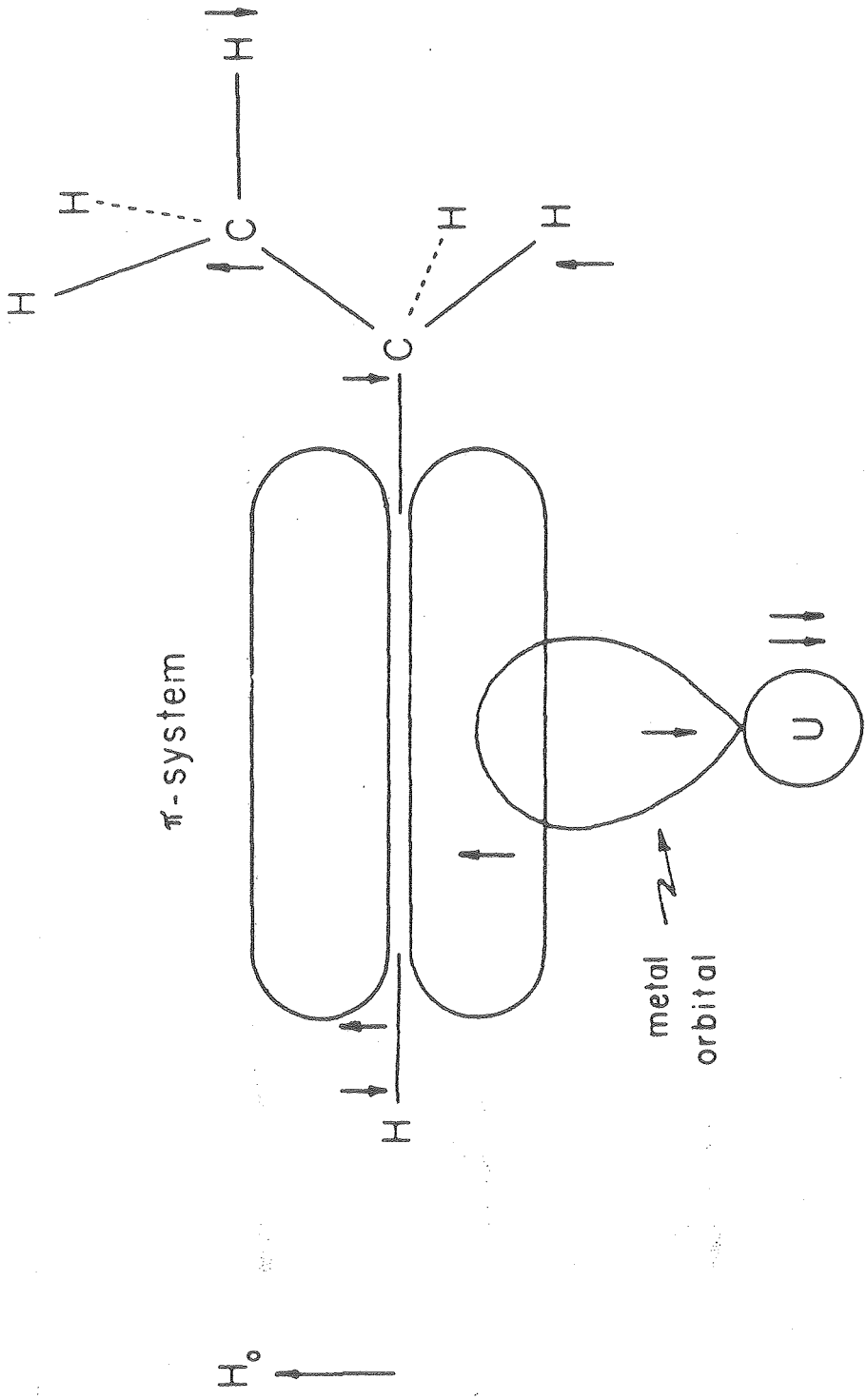

XBL 801-7889

Figure 2

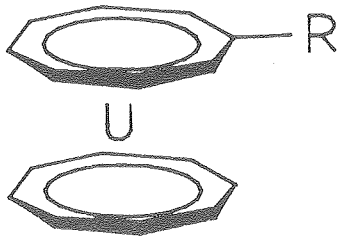

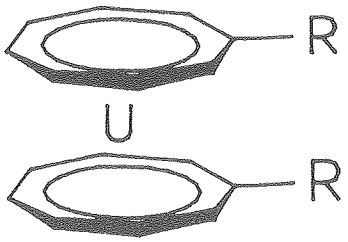

26, R=H
32, R=C(CH$_3$)$_3$
42, R=COOC(CH$_3$)$_3$

27, R=CH$_3$
28, R=CH$_2$CH$_3$
29, R=(CH$_2$)$_3$CH$_3$
30, R=CH(CH$_3$)$_2$
31, R=CH$_2$C(CH$_3$)$_3$

33, R=C(CH$_3$)$_3$
36, R=C$_6$H$_5$
37, R=p-C$_6$H$_4$NMe$_2$
41, R=COOC(CH$_3$)$_3$
43, R=C$_8$H$_7$

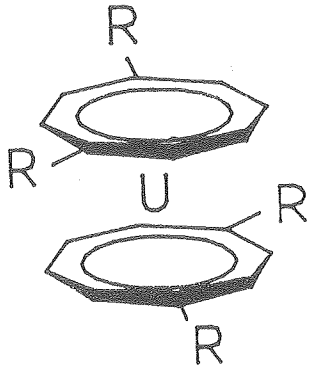

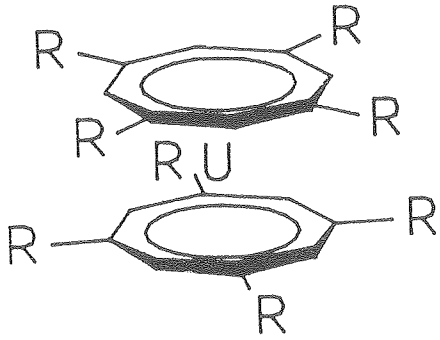

34, R=C(CH$_3$)$_3$

35, R=CH$_3$

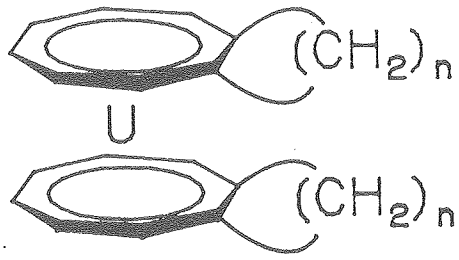

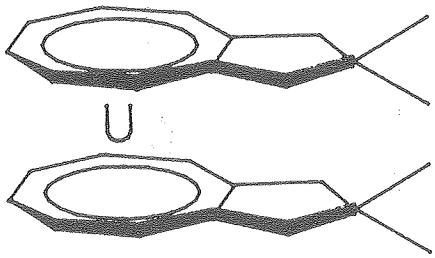

38, n=2
39, n=3
44, n=4

40

Figure 3

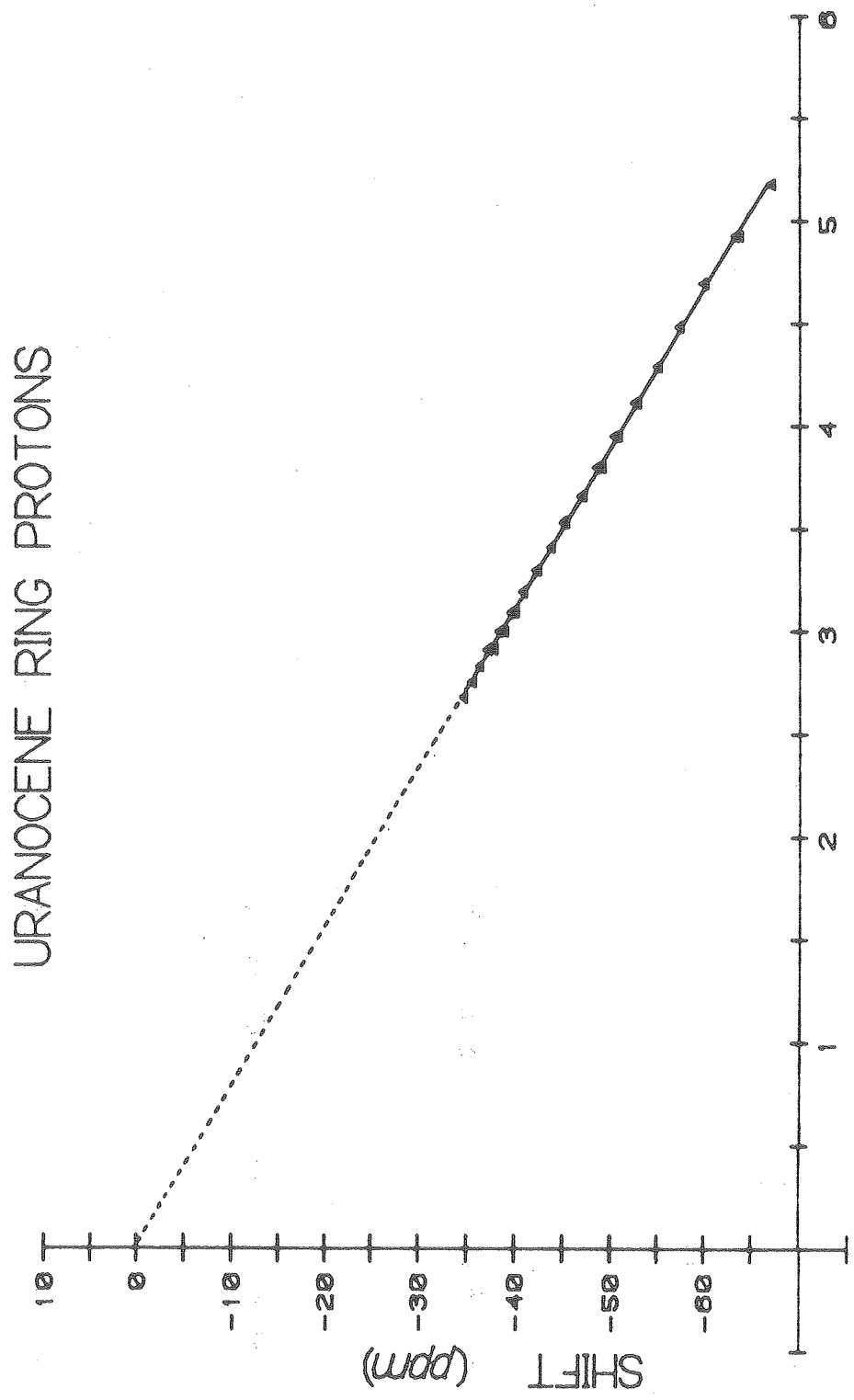

XBL 801-7890

Figure 4

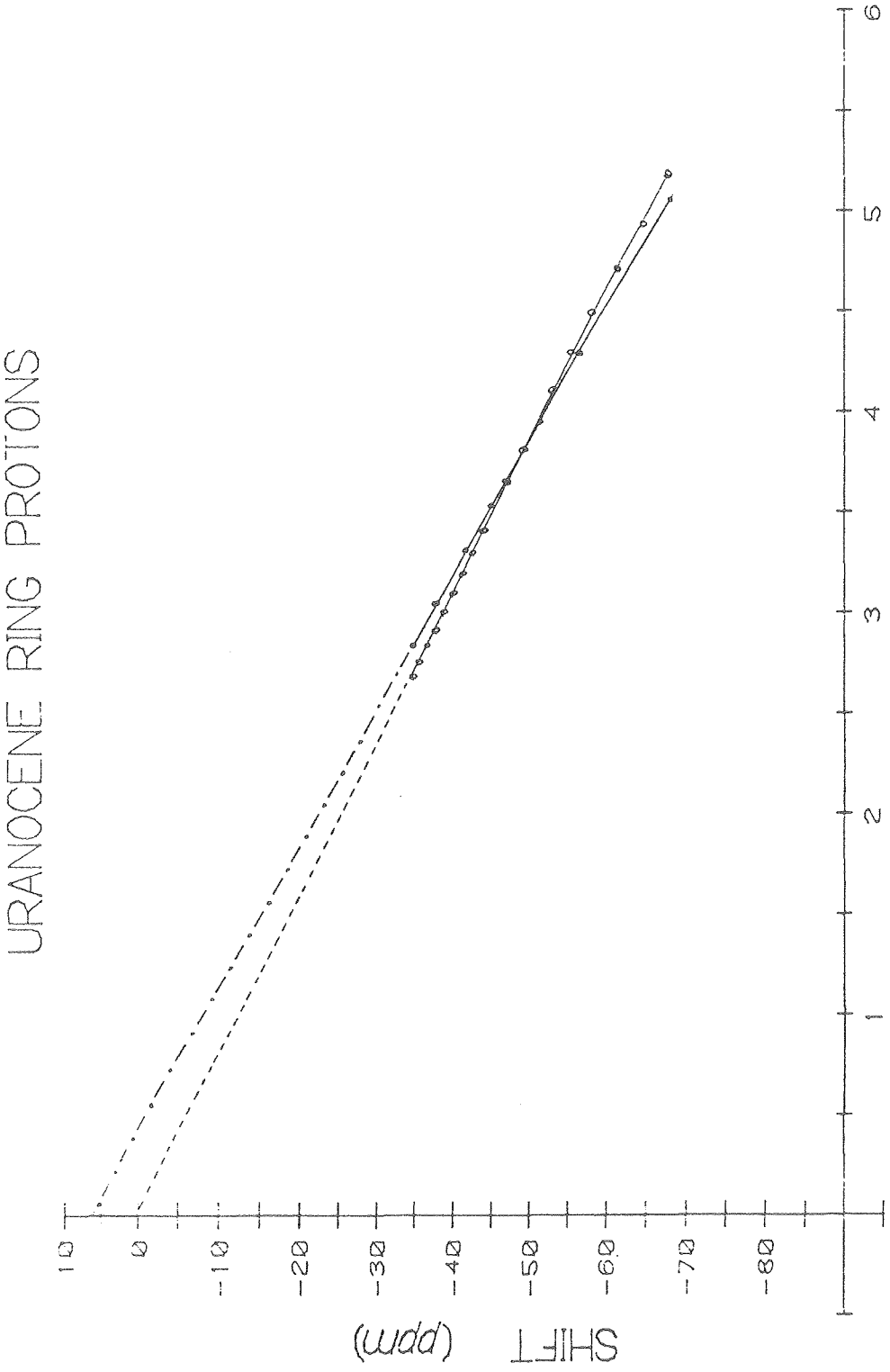
URANOCENE RING PROTONS
SHIFT (ppm)
10
0
-10
-20
-30
-40
-50
-60
-70
-80
1/T x 1000 (°K)
1
2
3
4
5
6

Figure 5

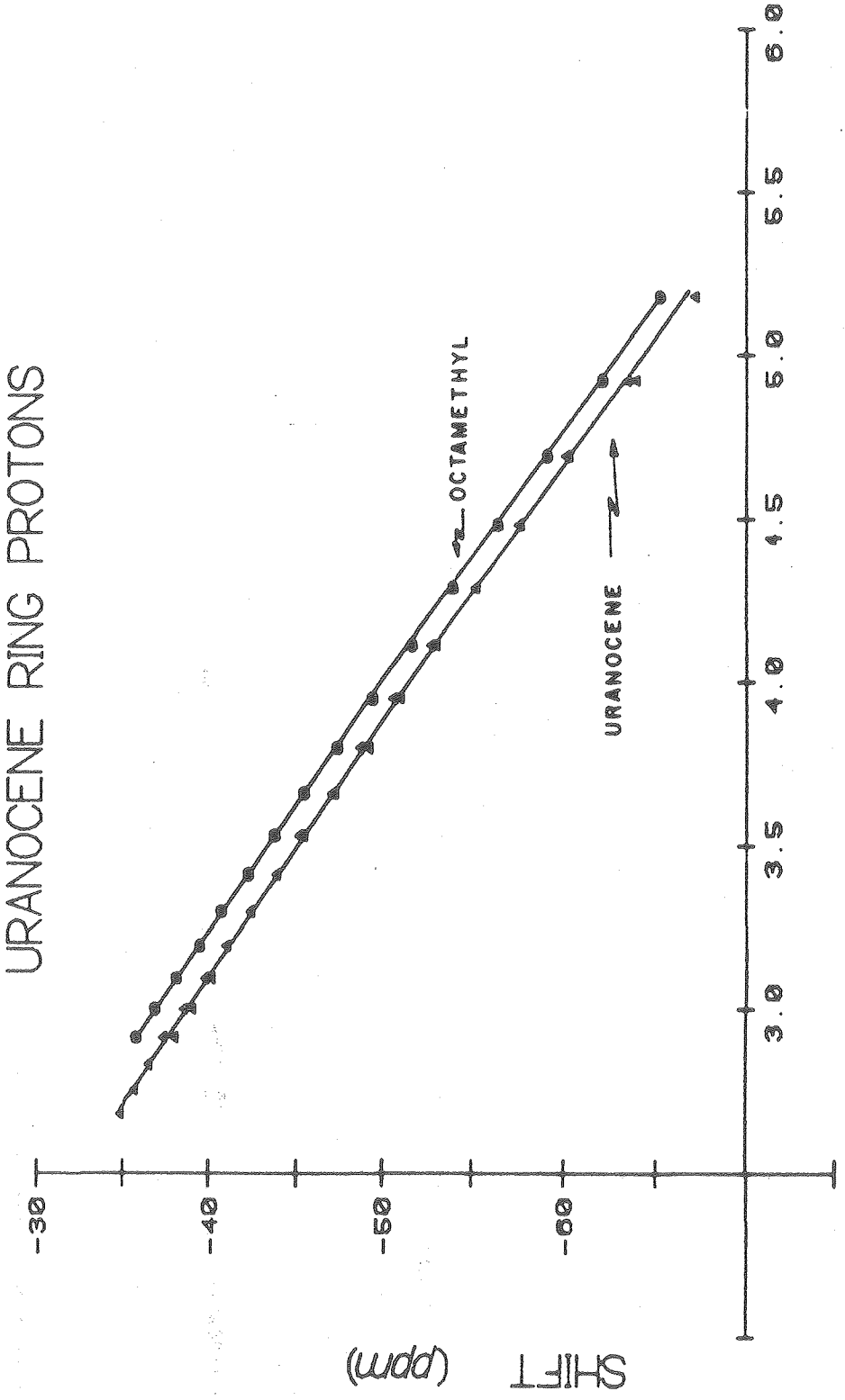

XBL 801-7891

Figure 6

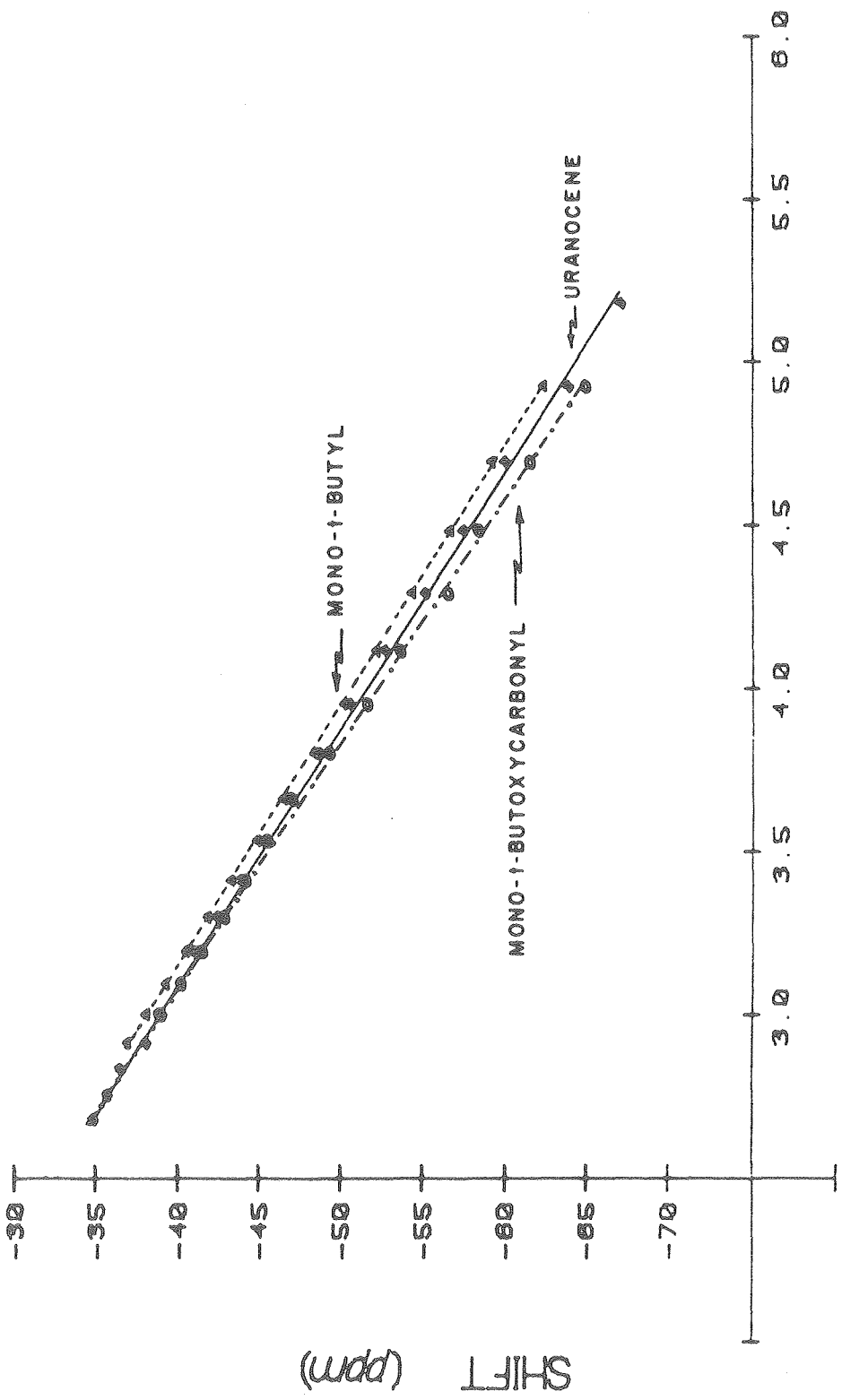

XBL 801-7892

Figure 7

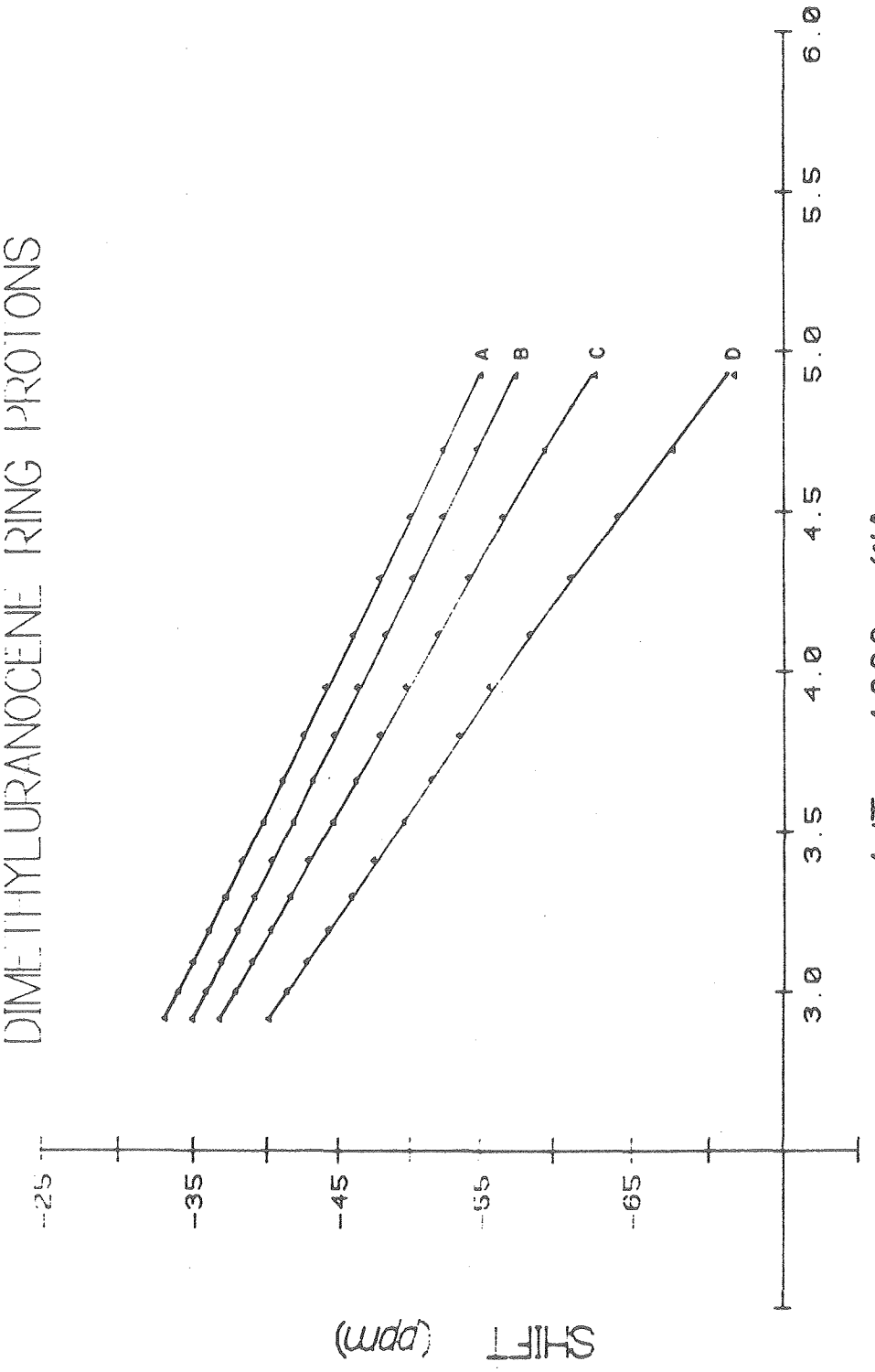

XBL 7912-13544

Figure 8

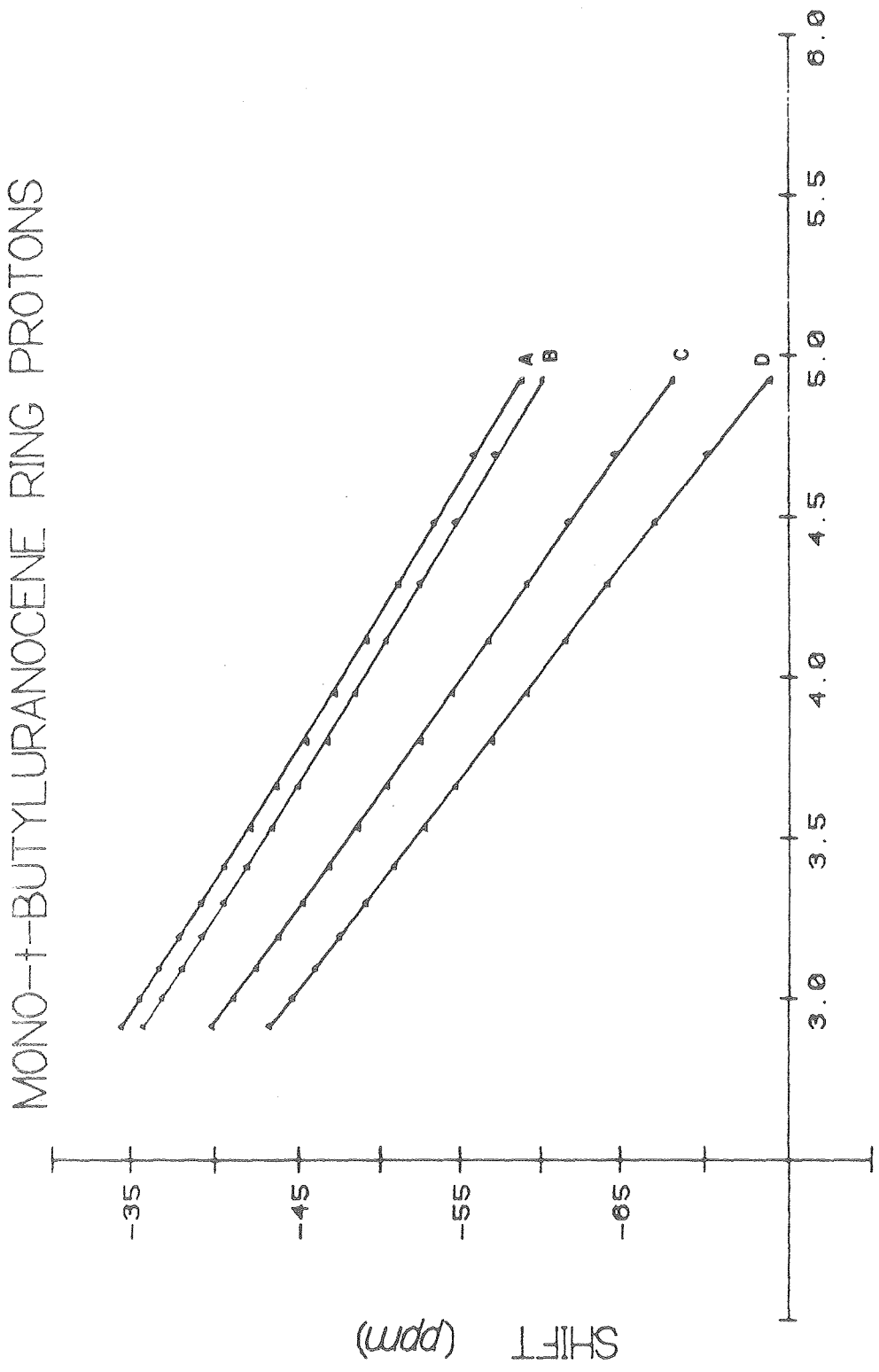

XBL 801-7893

Figure 9

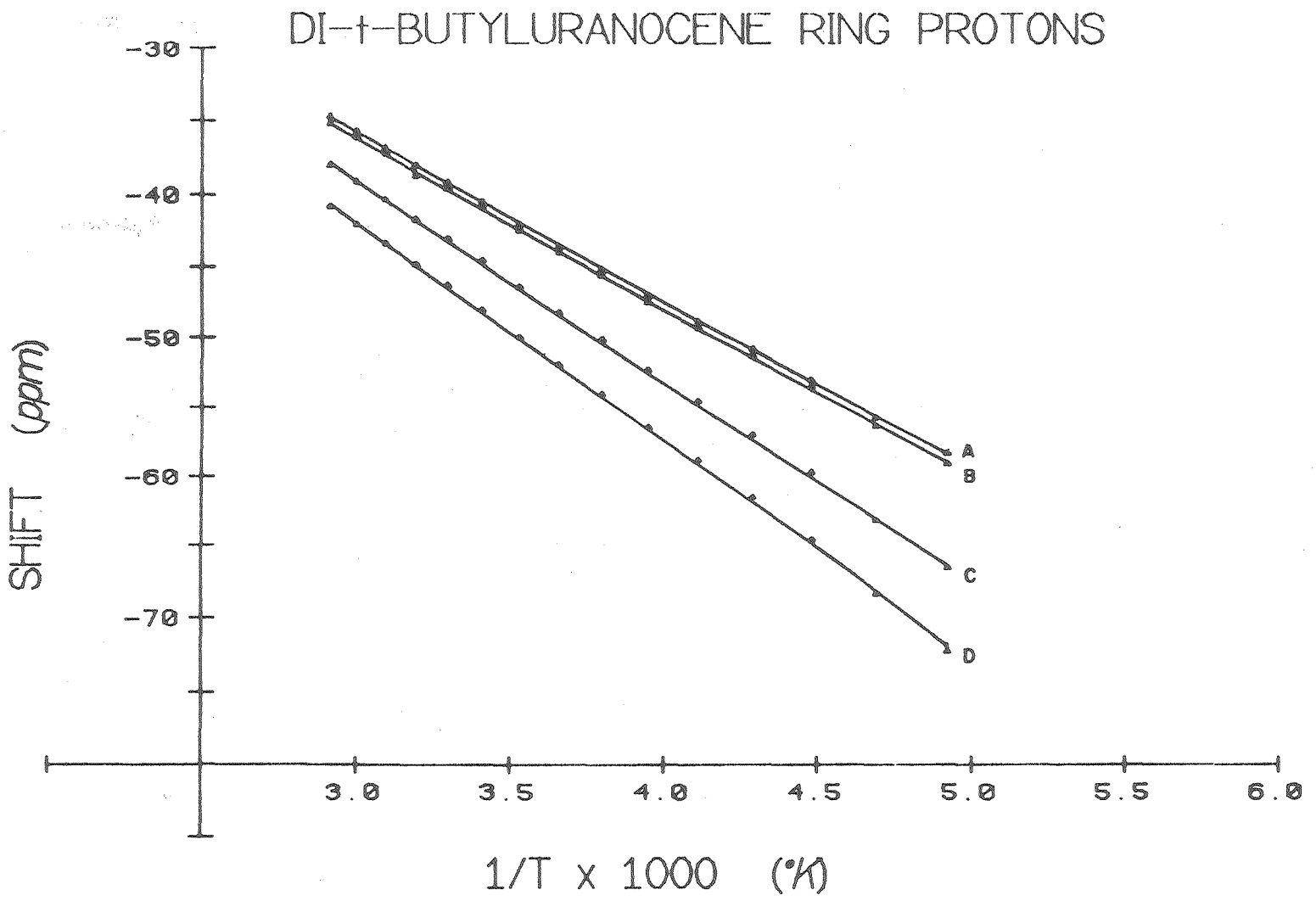

XBL 801-7894

Figure 10

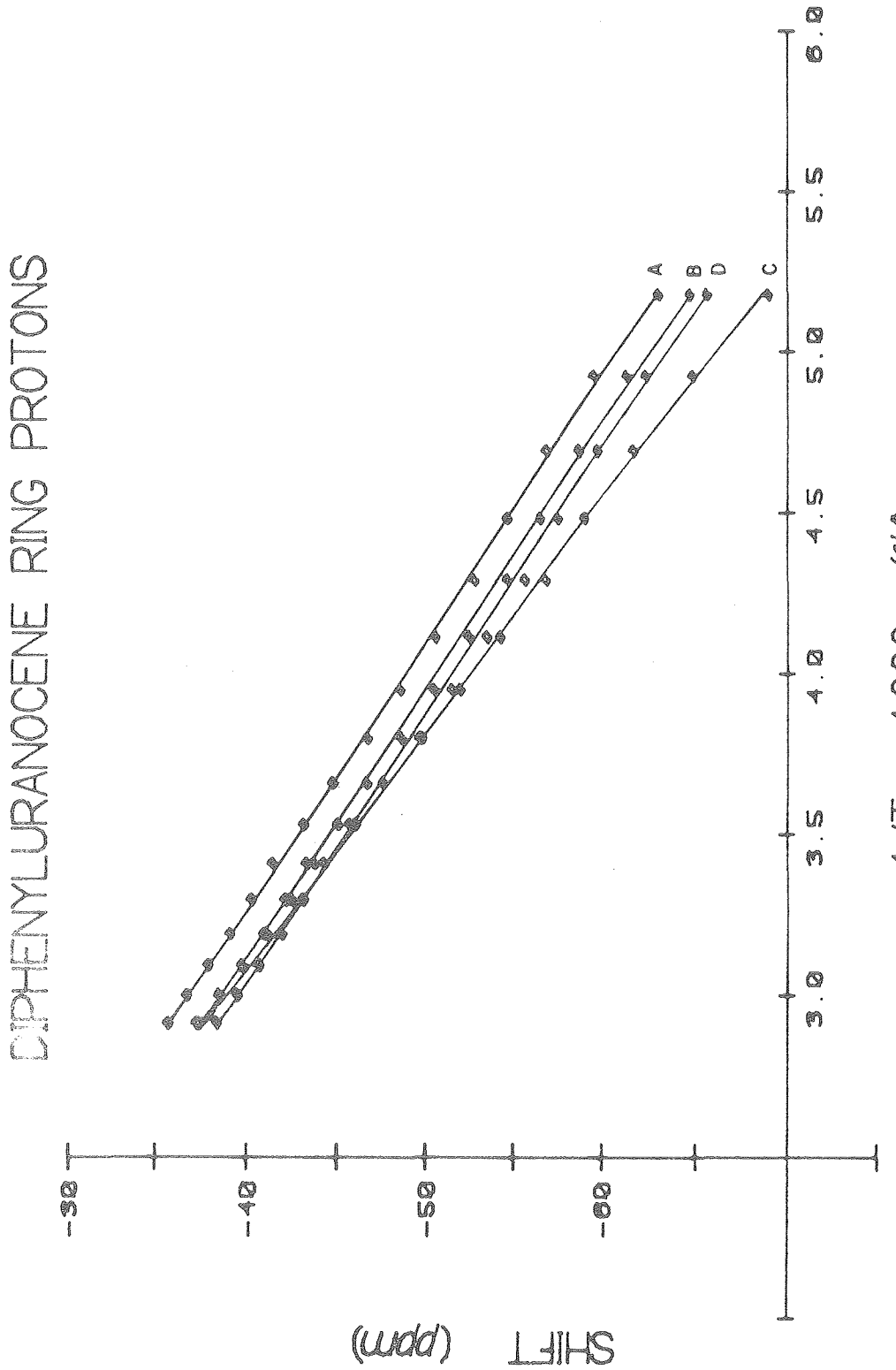

XBL 801-7896

Figure 11

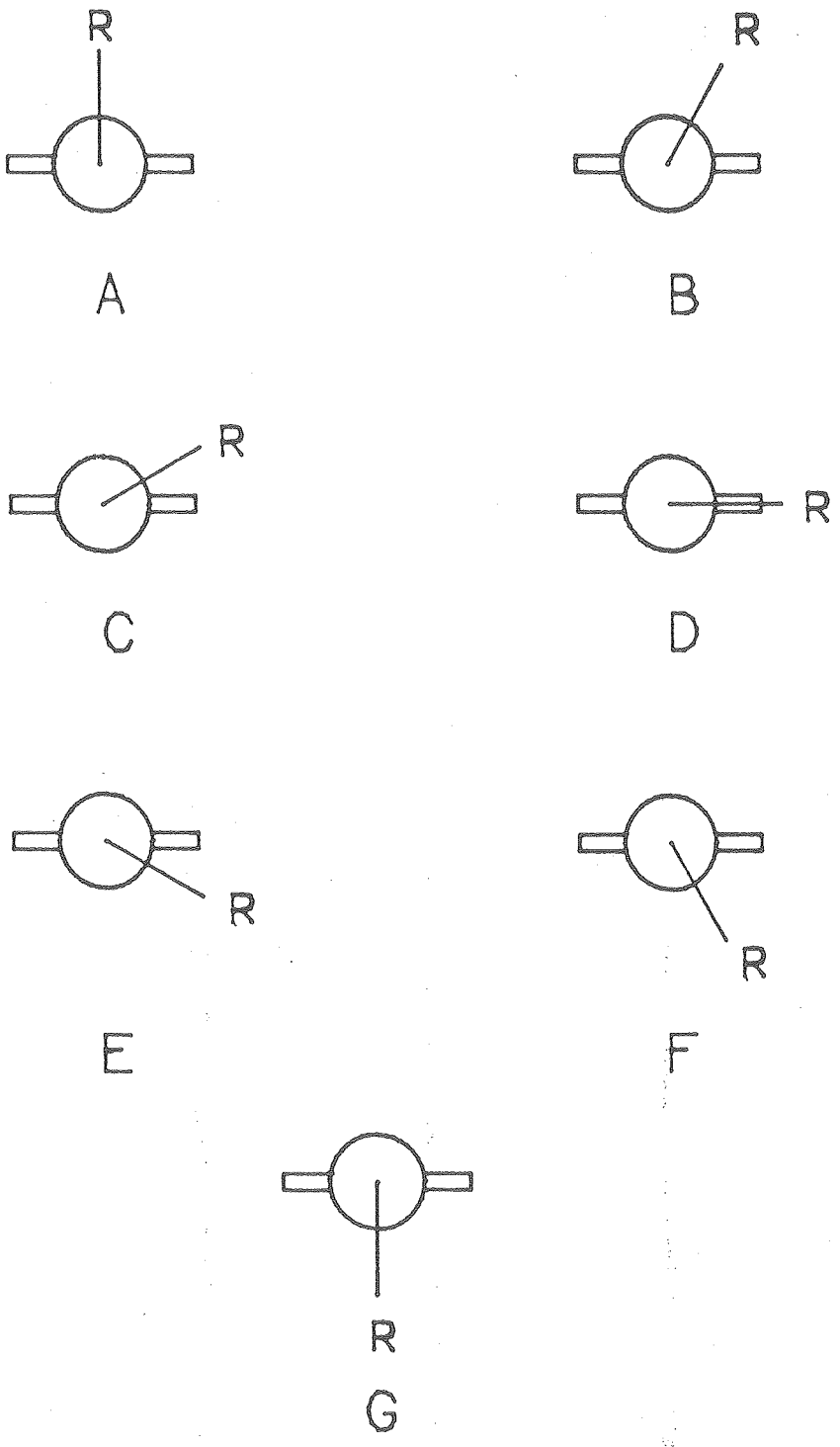

XBL 801-7887

Figure 12

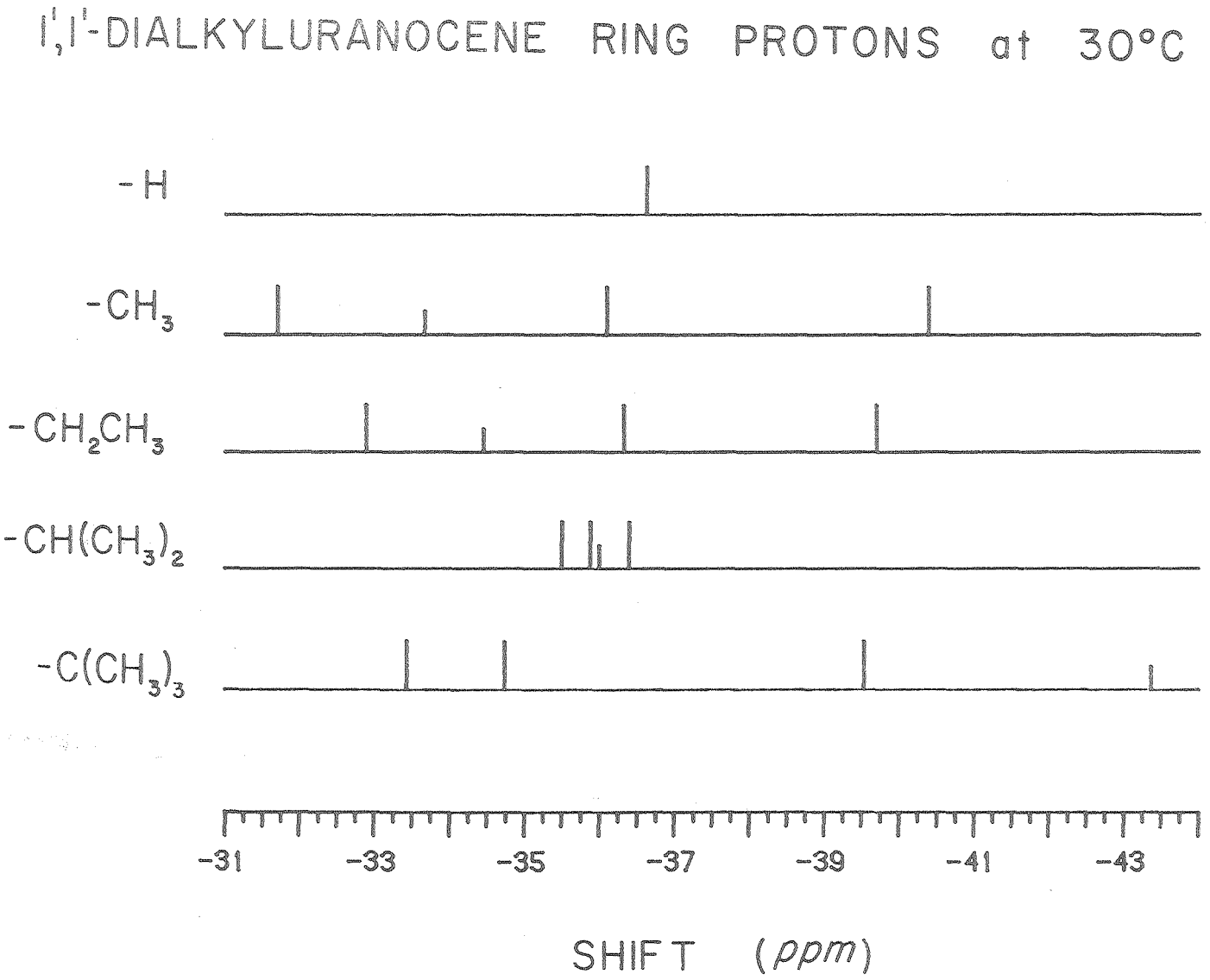
1',1'-DIALKYLURANOCENE RING PROTONS at 30°C
-H
-CH3
-CH2CH3
-CH(CH3)2
-C(CH3)3
-31
-33
-35
-37
-39
-41
-43
SHIFT (ppm)
XBL 7912-13545

Figure 13

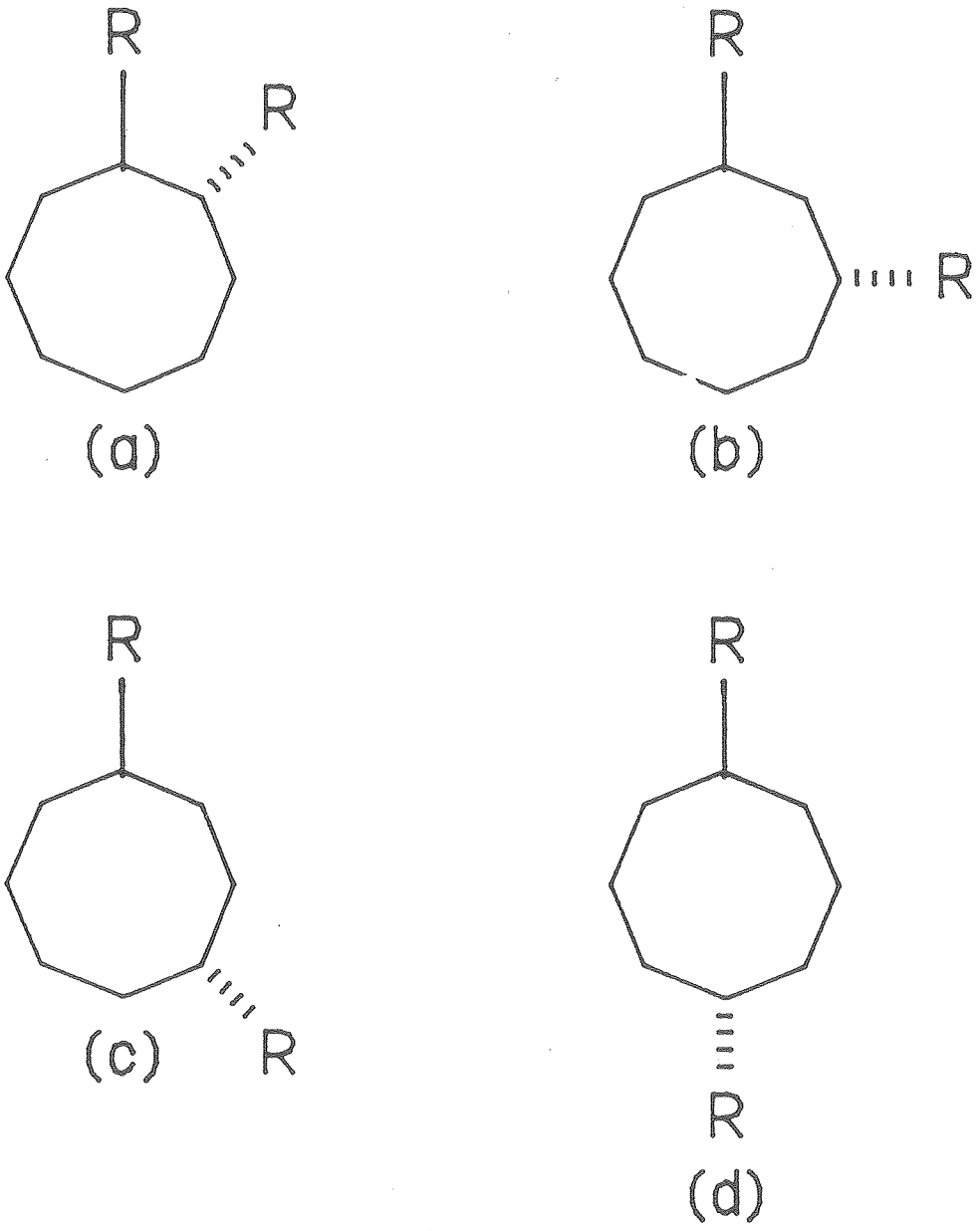

XBL 801-7886

Figure 14

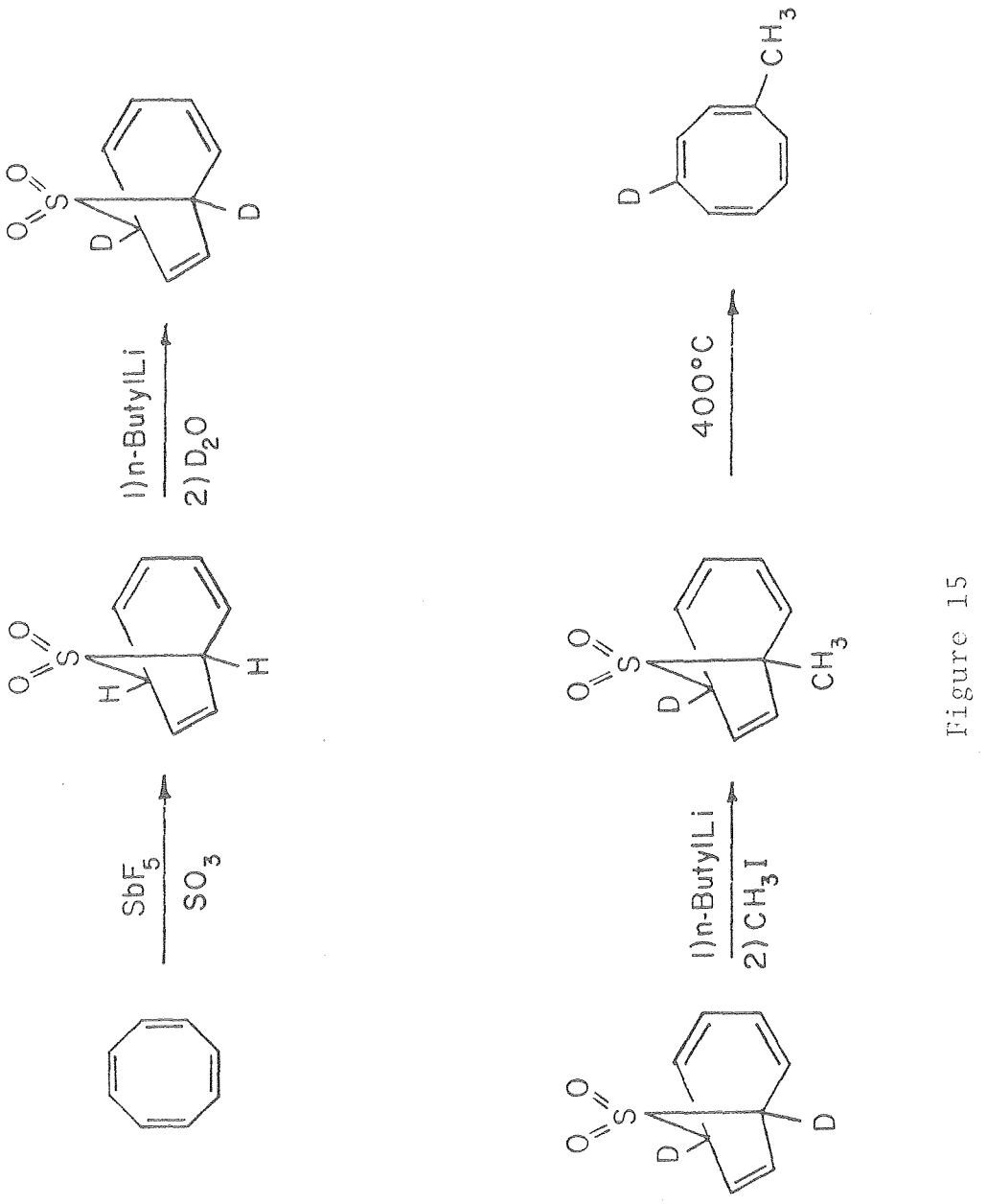

Figure 15

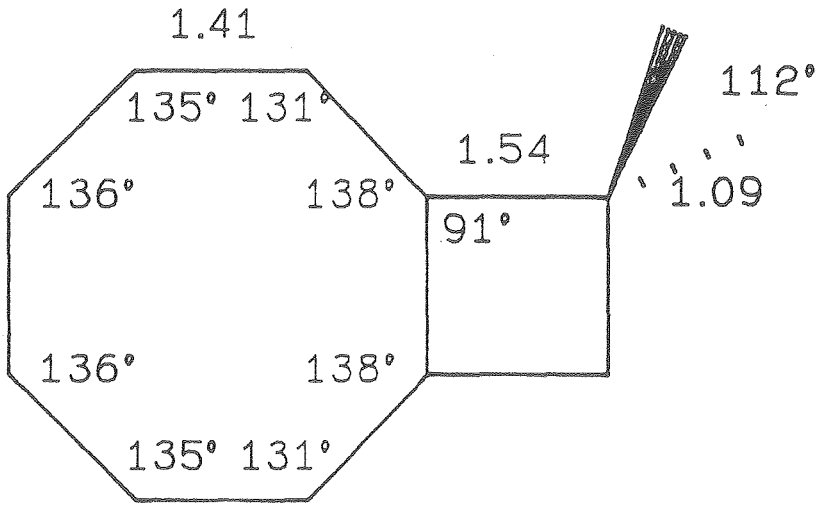

Figure 16